



## King's Research Portal

DOI:

[10.1002/esp.4494](https://doi.org/10.1002/esp.4494)

*Document Version*

Peer reviewed version

[Link to publication record in King's Research Portal](#)

*Citation for published version (APA):*

Gurnell, A. M., Bertoldi, W., Francis, R. A., Gurnell, J., & Mardhiah, U. (2018). Understanding processes of island development on an island braided river over timescales from days to decades. *EARTH SURFACE PROCESSES AND LANDFORMS*. <https://doi.org/10.1002/esp.4494>

### Citing this paper

Please note that where the full-text provided on King's Research Portal is the Author Accepted Manuscript or Post-Print version this may differ from the final Published version. If citing, it is advised that you check and use the publisher's definitive version for pagination, volume/issue, and date of publication details. And where the final published version is provided on the Research Portal, if citing you are again advised to check the publisher's website for any subsequent corrections.

### General rights

Copyright and moral rights for the publications made accessible in the Research Portal are retained by the authors and/or other copyright owners and it is a condition of accessing publications that users recognize and abide by the legal requirements associated with these rights.

- Users may download and print one copy of any publication from the Research Portal for the purpose of private study or research.
- You may not further distribute the material or use it for any profit-making activity or commercial gain
- You may freely distribute the URL identifying the publication in the Research Portal

### Take down policy

If you believe that this document breaches copyright please contact [librarypure@kcl.ac.uk](mailto:librarypure@kcl.ac.uk) providing details, and we will remove access to the work immediately and investigate your claim.

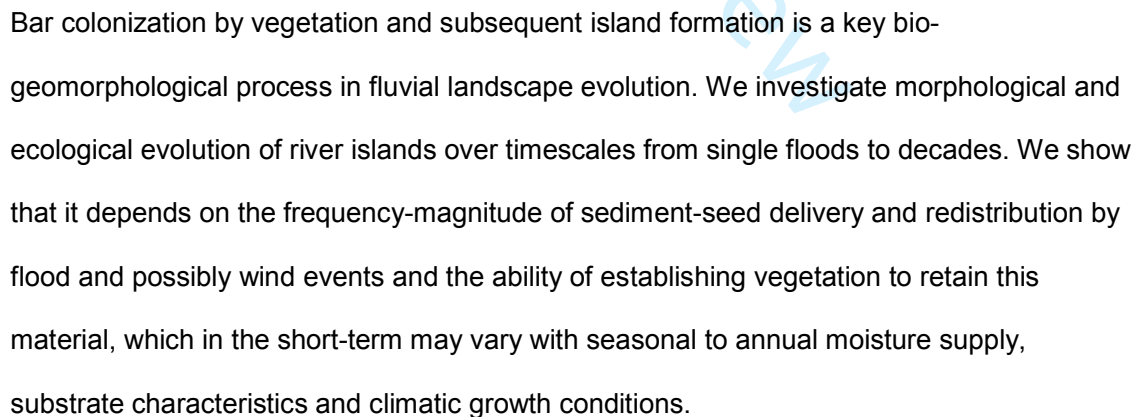
# Earth Surface Processes and Landforms

## Understanding processes of island development on an island braided river over timescales from days to decades

Journal:	<i>Earth Surface Processes and Landforms</i>
Manuscript ID	ESP-17-0489.R2
Wiley - Manuscript type:	Special Issue Paper
Date Submitted by the Author:	n/a
Complete List of Authors:	Gurnell, Angela; Queen Mary, University of london, Geography Bertoldi, Walter; Universita degli Studi di Trento, Ingegneria Civile Ambientale e Meccanica Francis, Robert; King's College London, Geography Gurnell, John; Queen Mary, University of london, Biological and Chemical Sciences Mardhiah, Ulfah; Freie Universität Berlin, Institut für Biologie, Plant Ecology
Keywords:	river islands, biogeomorphology, fluvial processes, riparian vegetation, wind

SCHOLARONE™  
Manuscripts

Angela M. Gurnell, Walter Bertoldi, Robert A. Francis, John Gurnell, Ulfah Mardhiah



**Understanding processes of island development on an island braided river over timescales from days to decades**

**Short title: Understanding processes of island development**

Angela M. Gurnell<sup>1\*</sup>, Walter Bertoldi<sup>2</sup>, Robert A. Francis<sup>3</sup>, John Gurnell<sup>4</sup>, Ulfah Mardhiah<sup>5,6</sup>

1 School of Geography, Queen Mary University of London, Mile End Road, London E1 4NS, United Kingdom.

2 Department of Civil, Environmental and Mechanical Engineering, University of Trento, Via Mesiano 77, 38123 Trento, Italy

3 Department of Geography, King's College London, Strand Campus, London WC2R 2LS, United Kingdom

4 School of Biological and Chemical Sciences, Queen Mary University of London, Mile End Road, London E1 4NS, United Kingdom.

5 Institut für Biologie, Plant Ecology, Freie Universität Berlin, Altensteinstr. 6, D-14195, Berlin, Germany

6 current address: Wildlife Conservation Society - Indonesia Program. Jl. Tampomas No. 35, Bogor, 16151, West Java, Indonesia.

\* Corresponding author: a.m.gurnell@qmul.ac.uk

**ABSTRACT**

Bar colonization by vegetation and subsequent island formation is a key biogeomorphological process in fluvial landscape evolution. Here we investigate morphological and ecological evolution of river islands over timescales from single floods to decades, focussing on islands initiated by deposited trees that sprout to form vegetated patches.

On a braided reach of the high-energy Tagliamento River, Italy, we monitored 30 pioneer islands of 1-17 years age in comparison with unvegetated bar surfaces, open areas between

1  
2  
3  
4  
5  
6  
7  
8  
9  
10  
11  
12  
13  
14  
15  
16  
17  
18  
19  
20  
21  
22  
23  
24  
25  
26  
27  
28  
29  
30  
31  
32  
33  
34  
35  
36  
37  
38  
39  
40  
41  
42  
43  
44  
45  
46  
47  
48  
49  
50  
51  
52  
53  
54  
55  
56  
57  
58  
59  
60

islands, and established islands surfaces. We integrated morphological, surface sediment and vegetation properties of islands initiated by different flood events, combining evidence from remotely-sensed and ground observations, flow and climate time series.

At a decadal time scale, pioneer islands aggrade rapidly to the elevation of the mean annual flood, showing a steady increase in vegetation canopy height, fining of surface sediments from predominantly gravel to silty-sand with a notable clay and organic fraction. The standing vegetation included over 130 species, with the largest number on island surfaces of intermediate elevation and flood disturbance. As islands age, standing vegetation becomes comprised mainly of competitor species with transient seed banks and typical of woodland, scrub, pasture and wetland habitats, whereas the winter seedbank is dominated on all surfaces by ruderal species with persistent seedbanks, mainly associated with aquatic, wetland, pasture, arable and wasteland habitats. At shorter timescales, the bio-geomorphological trajectory of pioneer islands is initiated by large flood events that control the elevation of deposited trees, and subsequent flows that control tree survival and establishment. Island morphological evolution depends on the frequency-magnitude of sediment and seed delivery and redistribution by flood and possibly wind events, whereas island ability to retain sediments reflects the degree of vegetation establishment, which in the short-term may vary with seasonal to annual moisture supply, substrate characteristics and climatic growth conditions.

**KEY WORDS**

**river islands, biogeomorphology, fluvial processes, riparian vegetation, wind**

**INTRODUCTION**

Islands provide morphological and biological complexity to river environments (Ward et al., 2002b, Gurnell et al., 2005) and are an important element of river morphodynamics (Hupp and Osterkamp, 1996; Schnauder and Moggridge, 2009). Although the susceptibility of a river reach to island development depends primarily on physical setting and fluvial processes (e.g. Osterkamp, 1998, Osterkamp et al., 2001, Moretto et al., 2014, Perona et al., 2014, Baubinienė et al., 2015, Belletti et al., 2015), river islands develop within susceptible river reaches through interactions between vegetation and fluvial processes (Gurnell et al., 2001, 2012). Such interactions have been observed in the field (e.g. Corenblit et al., 2009, Wintenberger et al., 2015, Bywater-Reyes et al., 2017), through analysis of time sequences of aerial images (e.g. Bollati et al., 2015, Mardhiah et al., 2015, Corenblit et al., 2016) and in flume experiments (e.g. Bertoldi et al., 2015, Gran et al., 2015, Diehl et al., 2017).

Many different styles of island have been recognised and attributed to a variety of physical processes (e.g. Wyrick and Klingeman, 2011) but island development additionally reflects two broad types of interactions between vegetation and fluvial processes, either singly or in combination (Gurnell et al., 2001, 2012). ‘Building’ islands evolve as a result of the colonisation of mid-channel bars by vegetation and the further retention and stabilisation of sediment on the bars by vegetation. ‘Dissection’ islands are created by flows of water across pre-existing vegetated surfaces (e.g. floodplains, large islands), where the flow paths and the success of flows in dissecting the land surface depend to some degree on the distribution and type of vegetation that is present, and the degree to which root systems prevent or redirect the dissection and downcutting process. ‘Complex islands’ develop from some combination of these two processes.

In this paper we focus on ‘building’ islands, where vegetation colonisation and growth plays a pivotal role in the retention and stabilisation of materials that underpin the island’s aggrading morphology. Even in the lowest energy freshwater environments, retention and stabilisation of organic material, created by local vegetation under the influence of plant-groundwater-surface water interactions and related nutrient dynamics, underpins soil

1  
2  
3 78 formation and the topographic development of ‘tree islands’ (Wetzel, 2002). As flow energy  
4  
5 79 increases, interactions between plants and physical processes of mineral sediment transfer  
6  
7 80 and retention increasingly drive island development (Bertoldi et al., 2009). In addition, the  
8  
9 81 range of plant species that are able to grow sufficiently rapidly to remain anchored and avoid  
10  
11 82 uprooting or stripping by fluvial processes and to intercept, retain and stabilise organic and  
12  
13 83 mineral sediments, reduces as flow energy increases. Thus, in relatively low energy river  
14  
15 84 environments a range of both woody and non-woody plants can initiate island development  
16  
17 85 by retaining and stabilising mainly finer sediments. However, as flow energy increases,  
18  
19 86 plants that are able to engineer island development are predominantly woody. Furthermore,  
20  
21 87 whereas seedlings of woody plants grow sufficiently rapidly to initiate island development on  
22  
23 88 many rivers, in very high energy systems woody species that are able to propagate  
24  
25 89 vegetatively become the main island engineers because of their ability to rapidly sprout and  
26  
27 90 grow robust above- and below-ground biomass that can withstand strong shear stresses and  
28  
29 91 deep burial during flood events (Gurnell, 2014).  
30  
31 92 Here we build on a conceptual model of island development proposed by Gurnell et al.  
32  
33 93 (2001) that is applicable to high energy rivers of the northern temperate zone, where  
34  
35 94 Salicaceae species dominate the riparian woodland. The model envisages three phases of  
36  
37 95 building island development, from the deposition of entire uprooted trees and other living  
38  
39 96 large wood (i.e. capable of resprouting) on bar surfaces during the falling limb of flood  
40  
41 97 events, through an initial pioneer island phase of sprouting and sediment retention, to an  
42  
43 98 established island phase as a result of the aggradation, enlargement and coalescence of  
44  
45 99 pioneer islands. Since 2001, a number of refinements to the conceptual model have been  
46  
47 100 introduced (Gurnell and Petts, 2002; Gurnell et al., 2012, 2016), and empirical evidence has  
48  
49 101 been presented to support specific aspects of the model, including for example, island  
50  
51 102 morphological (Bertoldi et al., 2011), sedimentological (Gurnell et al., 2008), soil (Mardhiah  
52  
53 103 et al., 2014, Bätz et al., 2015), and vegetation development (Francis et al., 2008, Perona et  
54  
55 104 al., 2014); living wood recruitment and dynamics (Bertoldi et al., 2013); early growth rates of

tree seedlings, cuttings and deposited trees (Francis et al., 2005, 2006, Francis and Gurnell, 2006, Francis, 2007; Moggridge and Gurnell, 2009) and interactions among developing subsurface tree root and shoot biomass and sediment retention (Holloway et al., 2017 a, b, c). In this paper we integrate empirical evidence of the processes and forms that accompany island evolution over decadal to event timescales, focusing on a single island-braided river reach of the Tagliamento River, Italy. Specifically, we consider:

- (i) Trajectories of island topographic and vegetation canopy development based on the analysis of multi-temporal airborne Lidar data
- (ii) Trajectories of vegetation succession and surface sediment development based on field sampling and measurements conducted on island and inter-island surfaces of different age
- (iii) Short-term (seasonal, event) adjustments reflecting flow and surface sediment dynamics that may influence the longer-term trajectories identified in (i) and (ii)

## METHODS

The research was conducted on a reach of the **braided**, gravel-bed Tagliamento River, Italy (Figure 1). The Tagliamento is one of the few European rivers that maintains largely intact morphological and ecological dynamism and complexity along much of its length, and is therefore considered a reference river system for the Alps and a model system for large rivers (Tockner et al., 2003). The river runs 172 km from source to mouth and its climate varies from alpine to mediterranean. Most importantly for this research, it maintains river islands along several reaches, which have been the focus of a range of hydrogeomorphological and ecological investigations over the last two decades (see Gurnell, 2016). The island-braided reach focused on here (46°12' N, 12°59' E) is in the prealpine section (140 m a.s.l.) and has a wet mediterranean climate with a mean annual precipitation of approximately 2000 mm. Peak river flows are in spring (snowmelt) and autumn (rainfall).



1  
2  
3  
4  
5  
6  
7  
8  
9  
10  
11  
12  
13  
14  
15  
16  
17  
18  
19  
20  
21  
22  
23  
24  
25  
26  
27  
28  
29  
30  
31  
32  
33  
34  
35  
36  
37  
38  
39  
40  
41  
42  
43  
44  
45  
46  
47  
48  
49  
50  
51  
52  
53  
54  
55  
56  
57  
58  
59  
60

131 The water table at the study site showed subdued variation through the year as a result of  
132 groundwater upwelling induced by local narrowing of the river valley towards a gorge section  
133 approximately 2 km downstream.

134 Information was assembled from airborne Lidar surveys, river stage records, field campaigns  
135 and the laboratory analysis of field samples to investigate the morphological, surface  
136 sediment and vegetation evolutionary characteristics of islands within the study area. The  
137 timing of the Lidar surveys, tree deposition events that initiated the studied pioneer islands,  
138 and field measurement campaigns are plotted in relation to the January 2000 to February  
139 2017 time series of daily river stage (corrected to detrended elevations within the study  
140 reach, see below for correction method) in Figure 2.

141

142 **Lidar data, river stage and climate station records**

143 Three airborne Lidar surveys were available for analysis, captured in May 2005, August  
144 2010 and October 2013. The Lidar surveys covered the study reach and had a spatial  
145 resolution ranging from 1 (2005 survey) to approximately 10 points/m<sup>2</sup> (2013 survey). These  
146 were analysed to obtain tree canopy height and detrended surface elevations for all field  
147 sampling locations on surfaces of different age and type (see the following subsection on  
148 ‘Field sampling and measurements’).

149 The free software FUSION, developed by the U.S. Department of Agriculture, Forest  
150 Service, Remote Sensing Applications Center (available at <http://www.fs.fed.us/eng/rsac/>)  
151 was employed to filter the Lidar point cloud differentiating between ground points and  
152 vegetation points. From this information we obtained a Digital Elevation Model (DEM) and a  
153 Canopy Surface Model (CSM), with a spatial resolution of 2 m for 2005 and 1 m for 2010  
154 and 2013 (see Bertoldi et al., 2011 for further details). River bed and vegetation canopy  
155 elevations were extracted from these two raster data sets within circular areas of 5 m radius  
156 centred on the 2016/2017 field sampling locations. Since there was considerable flood

disturbance of lower areas of the river bed between October 2013, when the most recent Lidar data were captured, and 2014, when the trees initiating the youngest studied pioneer islands were deposited, analysis of the Lidar data was confined to sampling points on established islands (probably initiated in the mid to late 1970s, hereafter conservatively labelled 1980), pioneer islands initiated in 2000 and 2004, and surfaces between the 2000 and 2004 islands.

The extracted elevation data was detrended to remove the impact of the down-valley slope and thus highlight the relative cross-sectional river bed elevation of the sampling locations and sites. Detrending was achieved by computing a moving average of the 2005 DEM, based on an 800 m square window (800 m approximates the typical width of the active river corridor). Within each 800 m square window, areas outside of the active corridor were excluded when calculating the average bed elevation, which was then subtracted from all three DEMs to allow for a direct comparison of the temporal evolution of the different surfaces.

In order to explore the degree to which detrended surface elevation and vegetation canopy height varied across the different sampled surfaces, through time, and in relation to interactions between surfaces and time, generalised linear models were estimated to explore the dependence of vegetation canopy height and surface elevation on sampled surfaces, year of Lidar observation, and interactions between surface and year. The statistical significance of differences between particular surfaces, years and surface-year interactions were explored using the Bonferroni method ( $P < 0.05$ ).

River stage records from the Villuzza gauging station, located approximately 2 km downstream from the study reach, provided information on flow events and sequences to aid interpretation of the morphological, sedimentary and vegetation data sets that were collected. River stage at Villuzza was linked to the detrended bed surface elevation of the study reach using oblique photographs captured with a temporal resolution of one hour by applying the method described by Bertoldi et al. (2009) and further developed by Welber et

1  
2  
3 184 al. (2012). Inundation maps at different flow stage were compared to the 2010 and 2013  
4 185 DEMs to obtain a relationship that transformed the river stage measured at Villuzza into the  
5 186 detrended DEM elevation coordinates. This allowed the frequency of inundation of the  
6 187 sampled locations and sites, based on 2000-2017 daily maximum stage records, to be  
7 188 estimated as well as their potential inundation between the two sampling campaigns in 2016  
8 189 and 2017.

15 190 Air temperature, solar radiant energy exposure, precipitation and wind speed data from a  
16 191 climatological station at Osoppo, about 7 km upstream (North-East) of the study reach, was  
17 192 used to explore conditions relevant to the interpretation of field data. In particular, air  
18 193 temperature data were used to estimate accumulated Growing Degree Days (GDD) that  
19 194 could indicate likely vegetation development at the time of field surveys. GDD was estimated  
20 195 as follows:

28 196 
$$\text{accumulated GDD} = \sum_1^n \left( \frac{T_{max} + T_{min}}{2} - T_{base} \right)$$

31 197 Where Tmax and Tmin are the maximum and minimum temperature on each day, Tbase is  
32 198 10°C, 1 is 1<sup>st</sup> January and n is the Julian day for which the estimate is required. This was  
33 199 complemented by analysis of accumulated solar radiant energy exposure.

37 200 Wind speed and precipitation data were combined with river stage information from the  
38 201 Viluzza gauge to explore climate conditions between field surveys.

42 202

45 203 **Field sampling and measurements**

47 204 Several types of sampling and measurement were undertaken in the field.

50 205 Surface sediments were sampled from 14<sup>th</sup> to 17<sup>th</sup> June 2016 and 22<sup>nd</sup> to 23<sup>rd</sup> February 2017  
51 206 to investigate their calibre, organic content and viable seed content. Following previous  
52 207 detailed analysis of historical air photographs to confirm timing of tree deposition / island  
53 208 initiation and estimation of contemporary tree ages using dendrochronology (Mardhiah et al.,

2015), samples were taken from surfaces of known age representing established islands (EI) initiated in the mid to late 1970s (1980EI); pioneer islands (PI) initiated during floods in late 2000, 2004 and 2014 (2000PI, 2004PI, 2014PI); areas between (btwn) 2000 and 2004 pioneer islands (2000btwn, 2004btwn) and across the unvegetated surface of gravel bars (unveg). Sampling on 2000, 2004 and 2014 pioneer islands centred on the largest central tree (2000PI, 2004PI) or a central point along the deposited tree (2014PI); the largest (oldest) trees on established islands (1980EI); locations close to the sampled pioneer islands but not on island surfaces (2000btwn, 2004btwn) and randomly located locations on unvegetated bar surfaces (unveg). In each case a cylindrical, 6 cm diameter sediment subsample was taken to a depth of 5 cm at the central location and at approximately 5m upstream, downstream and to either side of this central location. Where sampled pioneer islands were less than 10 m in either length or width, sub-samples were taken as far as possible from the centre up to a distance of 5 m but within the morphological limits of the island. A single aggregate sample was generated for each sampling location by combining these five subsamples. Aggregate samples were obtained from ten different sampling locations (Figure 1) for each of the surfaces of different age (1980EI, 2000PI, 2004PI, 2014PI, 2000btwn, 2004btwn, unveg). This yielded a total of 70 aggregate samples for June 2016 and 69 for February 2017 (one 2014 pioneer island was removed by an intervening flood and so could not be sampled). Although islands exhibit high vertical heterogeneity and distinct layering of sediments as a legacy of past disturbance events, previous investigations of sediment profiles to depths of over 1.5 m below the surface of established islands have revealed a weak upward fining of sediments, typically with a distinct sand and finer layer at the surface (for example, see profiles illustrated in Holloway et al., 2017b). In the present analysis, we focused on the top 5cm of sediment as this is not only indicative of the most recent sediment deposition but, as a consequence, it is most likely to contain viable propagules, recently deposited through local seed fall, anemochory or hydrochory. It is also the most relevant to plant germination. Furthermore, seed bank studies are typically conducted on samples taken to a depth of 5 cm (Thompson et al., 1997).

1  
2  
3 237 In addition to sampling **surface** sediments, in June 2016 the height of the 2000PI and 2004PI  
4  
5 238 central trees was also measured using a clinometer, and a vegetation survey was conducted  
6  
7 239 at 5 of the sampling locations (area approximately 10m x 10m) on each of the island  
8  
9 240 surfaces of different age (1980EI, 2000PI, 2004PI, 2014PI). Information was also available  
10  
11 241 from a vegetation survey conducted in July 2011 using the same methodology. This survey  
12  
13 242 focussed on five 2000, five 2004 and five 2010 pioneer islands. The last were almost 1 year  
14  
15 243 old at the time of the 2011 survey and so provide a comparison with the 2014 pioneer  
16  
17 244 islands that were approximately 1.5 years old when surveyed in 2016.

18  
19 245

20  
21  
22 246 **Surface sediment analysis**

23  
24 247 Following field sampling, all the aggregate **surface** sediment samples were air dried and  
25  
26 248 passed through a 4 mm sieve at the field station to ensure retention of all viable seeds. The  
27  
28 249 weight of sediment and coarse organic material in the >4 mm fraction were separately  
29  
30 250 weighed at the field station and an approximate 300 g subsample of the <4 mm fraction was  
31  
32 251 transferred to a UK laboratory for organic matter and particle size analysis (described in this  
33  
34 252 section) and investigation of the soil seed bank (described in the following section).

35  
36  
37 253 In the laboratory, organic content of the <4 mm fraction of all 139 samples was determined  
38  
39 254 by loss on ignition, and the mineral particle size distribution was determined at a resolution  
40  
41 255 of 1  $\phi$  from -2  $\phi$  (4 mm) to -12  $\phi$  by sieving through 2 mm (-1  $\phi$ ) and 1 mm (0  $\phi$ ) sieves and  
42  
43 256 then passing a subsample of the <1 mm fraction through a laser sizer to identify the particle  
44  
45 257 size distribution below 1 mm (0  $\phi$ ).

46  
47 258 Multivariate analyses were used to investigate broad patterns in the values of six summary  
48  
49 259 properties of the surface sediments: %organic (of the total sample), D50 ( $\phi$ ), %gravel,  
50  
51 260 %sand, %silt, %clay (of the total mineral fraction). The six variable data set was analysed  
52  
53 261 using Agglomerative Hierarchical Cluster Analysis (AHC) with Euclidean distance as the  
54  
55 262 distance measure and Ward's clustering algorithm. The number of clusters that most

effectively summarised variations in the samples was selected using the AHC agglomeration schedule plot coupled with an analysis of the statistical significance of differences among the six **surface** sediment properties between the clusters. The statistical significance of differences between clusters was assessed using Kruskal Wallis tests followed by multiple pairwise comparisons using Dunn's procedure with Bonferroni correction of the significance level. This non-parametric test was selected because most of the variables were measured on a percentage scale, and thus values were confined to the range 0 to 100.

Principal Components Analysis (PCA) was also applied to the six **surface** sediment property data set to assess whether any broad gradients were present in the data that could support interpretation of contrasts between the sampled surfaces of different age and type. Because most of the **surface** sediment properties were expressed as percentages, the PCA was performed on a (non-parametric) rank correlation matrix. In order to illustrate contrasts between the **surface** sediment classes identified by AHC, samples were coded by sediment cluster or class on a scatter plot of each sample's score on the first two PCs.

An average distribution for each surface age and sampling date (i.e. averages of ten particle size distributions) was calculated for particle size distributions for the <1mm ( $\phi$ ) mineral fraction (i.e. coarse sand and finer), which was entirely analysed by laser sizer. Overlays of the average distributions were used to explore changes in the composition of the mineral sediment in this coarse sand and finer fraction between sampling dates on the surfaces of different age. The differences between groups of particle size distributions drawn from different surfaces on two sampling dates (June 2016, February 2017) were investigated by estimating generalised linear models for each of the ten, fifty and ninety percentiles (D10, D50, D90) of the particle size distributions, using sampling year (2016, 2017), surface (1980EI, 2000PI, 2000btwn, 2004PI, 2004btwn, 2014PI, unveg) and interactions between year and surface as the explanatory variables. The percentile values were estimated using Gradistat software (Blott and Pye, 2001) and are expressed in  $\phi$  units. The statistical

1  
2  
3  
4  
5  
6  
7  
8  
9  
10  
11  
12  
13  
14  
15  
16  
17  
18  
19  
20  
21  
22  
23  
24  
25  
26  
27  
28  
29  
30  
31  
32  
33  
34  
35  
36  
37  
38  
39  
40  
41  
42  
43  
44  
45  
46  
47  
48  
49  
50  
51  
52  
53  
54  
55  
56  
57  
58  
59  
60

significance of differences between groups was established using the Bonferroni method  
( $P < 0.05$ ).

**Standing vegetation and soil seed bank analysis**

The viable seed bank contained in the February 2017 surface sediment samples was quantified using germination trials. By gathering surface sediments in February, only the more persistent seed bank was sampled, since few species produce seeds during winter. Subsamples of 60 gms weight were extracted from the <4 mm fraction of the aggregated surface sediment samples from each sampling location and were refrigerated (*circa* 4°C) on arrival at the laboratory. These were stored until June 2017, when a 10 week germination trial was conducted in outdoor poly-tunnels. No artificial lighting or heating was used in the tunnels. The sediment subsamples were sprinkled onto 3 cm deep sterile soil (John Innes #2) in 10 cm x 20 cm seed trays. The seed trays were watered regularly to maintain the soil at field capacity, and the trays were rearranged in the poly-tunnels at the end of each week to randomise germination conditions. As seeds germinated, the seedlings were identified to species and then removed from the trays. In some cases the seedlings were transferred to individual pots and grown on to support species identification. From these data, the number of viable seeds per m<sup>2</sup> and seed species composition were estimated for each sample. In order to compare with other living components of organic material in the sampled sediments, information on seed abundance (seeds per m<sup>2</sup>) in the February 2017 seedbank was compared with information on root and hyphal length collected across islands of different age (1980, 2000, 2004, 2010) and unvegetated bar surfaces (unveg) during May 2012 (for analytical methods see Mardhiah et al., 2014).

The standing vegetation was also surveyed on two occasions. Between 18 and 20 June 2016, the standing vegetation was recorded on five pioneer island and established island surfaces of different age (2014PI, 2004PI, 2000PI, 1980EI). A walk over survey was



conducted within the approximate 10m by 10m area from which surface sediment samples were taken and the presence of plant species was recorded within a search period of up to 1 hour. A survey of the standing vegetation was also conducted between 22 and 25 July 2011 using exactly the same methods as in June 2016, although only pioneer islands were surveyed. Five randomly selected pioneer islands dating from each of 2000, 2004 and 2010 (close to 1 year old at the time of survey) were surveyed.

Using information from Hodgson et al. (1995), the seed bank type (i.e. transient, short-term persistent, long-term persistent), most common terminal habitat, and functional type (Grime et al., 2007) were identified for as many of the species recorded in the standing vegetation and seed bank as was possible. For functional type, a score between 0 and 1 was assigned to C (competitor), S (stress-tolerator) and R (ruderal) components of the CSR functional type for each species (Hunt et al., 2004) to allow quantitative comparisons between sampling locations and between the species found in the two standing vegetation surveys and the seedbank germination trial. These properties of the standing vegetation and seedbank were then displayed using bar graphs to explore any apparent changes in the proportions of functional types present according to surface age. Similarities in the species composition of the standing vegetation and viable seed bank were assessed using Agglomerative Hierarchical Cluster analysis with the Jaccard coefficient as the similarity measure and clustering determined using the unweighted pair group average.

All statistical analyses presented in this paper were conducted using Minitab 18 or XLSTAT 2017.

336

## 337 RESULTS

### 338 Surface elevations and inundation frequency.

339 A generalised linear model revealed statistically significant variations in detrended river bed elevation across different surfaces and through the time sequence of Lidar surveys, but



1  
2  
3 341 there were no significant interactions between surfaces and time (Table 1). Bed elevations  
4  
5 342 were significantly higher in 2013 and 2010 in comparison with 2005, and the sampling sites  
6  
7 343 on the 1980 established island surfaces were significantly higher than the pioneer island and  
8  
9 344 between-island sampling sites initiated in 2000, which were in turn significantly higher than  
10  
11 345 surfaces initiated in 2004. However, there was high variance in the elevation of the pioneer  
12  
13 346 island and between island surfaces initiated in 2000 and 2004, and thus there was no  
14  
15 347 statistically significant difference in the elevation of the pioneer island and between island  
16  
17 348 surfaces initiated in either 2000 or in 2004.  
18  
19 349 The inter-quartile ranges in the detrended elevation of sampling locations on the 1980, 2000  
20  
21 350 and 2004 surfaces are illustrated in Figure 3 in relation to the water level duration curve  
22  
23 351 (estimated from 2000-2017 daily maximum stage records at Viluzza). The interquartile  
24  
25 352 ranges indicate that at the time of the 2005 Lidar survey, the recently deposited 2004PI were  
26  
27 353 inundated between approximately 9 and 40 days each year, whereas the 2000PI were  
28  
29 354 inundated between 0.8 and 3 days per year and the 1980EI were sufficiently elevated that  
30  
31 355 they were not inundated by the 2 year return period flood. These large differences in  
32  
33 356 inundation frequency explain why the interquartile ranges indicate a clear increase in  
34  
35 357 detrended surface elevation of the 2004PI and 2004btwn sampling locations through time.  
36  
37 358 The upper quartile of these elevations reaches the lower quartile of the 2000PI and  
38  
39 359 2000btwn sampling locations by 2013. The maximum water stage reached between  
40  
41 360 sediment sampling campaigns in June 2016 and February 2017 is also indicated on Figure  
42  
43 361 3, showing that most of the 2004 sampling locations were inundated during this period,  
44  
45 362 whereas all of the 1980EI and most of the 2000PI and 2000btwn sampling locations were  
46  
47 363 not inundated.

48  
49 364

50  
51  
52 365 **Surface sediment composition**  
53  
54  
55  
56  
57  
58  
59  
60

AHC applied to six **surface** sediment properties (D50( $\phi$ ), %organic, %gravel, %sand, %silt, %clay) yielded six significantly different clusters, which characterised distinct sediment classes within the 139 aggregate samples that were analysed. The number of samples assigned to each class and the centroid values of each **surface** sediment property within the six classes are presented in Table 2 and the degree to which each of the six properties displayed by sediment samples assigned to each class displayed significant differences are also summarised in Table 2.

PCA identified two major gradients or PCs that together explained 93% of the variance in the six variable data set. Focussing on high ( $>0.7$  and  $<-0.7$ ) PC loadings (Table 3), PC1 describes a gradient of decreasing %gravel (high negative loading) and increasing %silt, %clay, %organic and median particle size (D50 in  $\phi$  units indicating sediment fining) (high positive loadings), whereas PC2 describes an independent gradient of increasing %sand.

The AHC and PCA results are combined in Figure 4, where they can be compared with the surface type, age and survey year relevant to each sample, displayed on a scatter plot of the sample scores on the first and second PCs identified in the PCA. These scatter plots indicate that samples drawn from unvegetated bar surfaces (unveg), between pioneer islands (2000btwn, 2004btwn) and from the youngest pioneer islands (2014PI) (Figure 4 (i)) are predominantly associated with gravel, gravel-sand and sand-gravel sediments (classes A, B, C, Figure 4 (iv)). The older pioneer (2004PI, 2000PI) and established (1980EI) islands show a range of surface sediment sizes from predominantly sand, through sand with some silt, to sand-silt sediments, with a progressive increase in the D50 (in  $\phi$  units, indicating sediment fining) and organic content (classes D,E,F, Figure 4 (iii)) with increasing surface age (Figure 4 (v)). There is also some evidence of a change in **surface** sediment characteristics between summer 2016 and late winter 2017 (Figure 4 (ii)), particularly a shift from sand towards silt and clay (Figure 4 (iii)) in the area on the right of the plot, where scores on PC1 exceed 0 (Figure 4 (ii)).

392 Focussing on the  $<1\text{mm}$  ( $>0\phi$ , coarse sand and finer) sediment fraction (Figure 5), which is  
393 the size fraction analysed entirely by laser sizer, the average particle size distribution for all  
394 surfaces appears to fine between June 2016 samples and February 2017 apart from those  
395 extracted from established island (1980EI) and unvegetated surfaces (Figure 5, compare A  
396 and C with B and D). The most pronounced changes are observed for the 2004PI, 2014PI  
397 and 2004btwn locations. The change for 2014PI is particularly noticeable, moving from a  
398 distribution that is very similar to the unvegetated (unveg) surfaces in 2016 to a distribution  
399 that is approaching that of the vegetated surfaces (2004PI, 2000PI, 1980EI) in 2017,  
400 indicating a fast evolution of these finer sediments on pioneer islands in their first 1 to 2  
401 years.

402 This apparent fining trend in the  $<1\text{mm}$  fraction is supported by box plots and generalised  
403 linear models for the D10, D50 and D90 percentiles (in  $\phi$  units) of the 10 individual particle  
404 size distributions within each of the surface and sampling time groups (Figure 5E, F and G).  
405 The generalised linear model for the coarsest percentile (D10, Table 4), explains 66% of the  
406 variance, with a statistically significant overall fining of sediment between years, a significant  
407 decrease in the D10 particle size between the older island surfaces (1980EI, 2000PI,  
408 2004PI), the youngest PI and oldest between island surfaces (2014PI, 2000btwn), and the  
409 youngest between island and unvegetated bar surfaces (2004btwn, gravel). There were no  
410 statistically significant interactions between surfaces and year. This is supported by the box  
411 plots (Figure 5E), which show little change between years apart from a slight hint of fining on  
412 the youngest island (2014PI) surfaces. The results from this analysis should be treated with  
413 a little caution because some estimated D10 values for the coarsest samples (mainly from  
414 2004btwn and unveg surfaces) fall between 0 and  $-1\phi$  (i.e. slightly larger than the less than  
415  $1\text{mm}$  ( $0\phi$ ) range of the analysed data). This is an artefact of the very large percentage of  
416 particles in the  $0$  to  $1\phi$  fraction in these relatively coarse samples, which have highly skewed  
417 frequency distributions. The model for D50 particle size is similar to that for D10 (Table 4,  
418 Figure 5F), explaining 62% of the variance, and revealing the same statistically significant

patterns in fining between years and surfaces with no statistically significant interactions between years and surfaces. However, the finest percentile (D90) reveals a more complex fining pattern (Figure 5G, Table 4). The generalised linear model explains 57% in the variance of D90. Once again there is a statistically significant overall fining of **surface** sediment between years. The older island surfaces (1980EI, 2000PI, 2004PI) are finer than the between island surfaces (2000btwn, 2004btwn), which are finer than the open, unvegetated surfaces (unveg). In addition, the youngest island surfaces (2014PI) are finer than the unvegetated bar surfaces (unveg). There are also some significant year-surface interactions within the D90 data. The older island surfaces in both years (1980EI, 2000PI, 2004PI) and the youngest island and between island surfaces (2014PI, 2000btwn, 2004btwn) in 2017 are finer than the between island surfaces (2000btwn, 2004btwn) in 2016 and the unvegetated surfaces (unveg) in both years. These results illustrate a stronger fining of between island and younger island (2014PI, 2000btwn, 2004btwn) surfaces than other surfaces between the two survey years.

A final investigated property of the **surface** sediments was the living organic material that they contain. Some living components are illustrated in Figure 6, including viable seeds per m<sup>2</sup> estimated from the February 2017 **surface** sediment samples (Figure 6B), and the fungal hyphae (Figure 6C) and root content (Figure 6D) estimated from samples extracted from different surfaces during May 2012 by Mardhiah et al. (2014). Each of the three graphs in Figures 6 B, C and D represents a snap shot of properties that vary greatly through time. However, it is interesting to note that while roots and hyphae, which are largely developed *in situ*, show a steady increase with surface age, seeds, which may be deposited locally but are also subject to transport and deposition by various agents (e.g. water, wind), show a more variable pattern with greatest abundance on the 2004PI surfaces at the time of sampling, whereas unvegetated surfaces show the lowest abundance.

444

## 445 **Vegetation**

1  
2  
3 446 Vegetation canopy height estimates from the three Lidar surveys (2005, 2010, 2013) and  
4  
5 447 field clinometer measurements (2016) are shown in Figure 6A. Clinometer measurements  
6  
7 448 were only made at the 2004PI and 2000PI sampling locations, where both the top of the  
8  
9 449 canopy and the underlying ground surface could be seen clearly from a single measurement  
10  
11 450 point and thus accurately measured. The two box plots for these 2016 field measurements  
12  
13 451 indicate a realistic increase from the earlier Lidar estimates for the same surfaces and  
14  
15 452 sampling locations, suggesting that the Lidar estimates of canopy height for the other three  
16  
17 453 dates are quite accurate. Overall the island surface data (1980EI, 2000PI, 2004PI)  
18  
19 454 presented in Figure 6A define a growth curve for the *P. nigra* dominated woodland within the  
20  
21 455 reach. This indicates rapid vertical growth of approximately 1m each year for at least the first  
22  
23 456 15 years, after which vertical growth reduces as this species approaches maturity. The data  
24  
25 457 also illustrate the development of some vegetation cover between pioneer islands.  
26  
27 458 A generalised linear model for vegetation canopy height reveals statistically significant  
28  
29 459 ( $P<0.05$ ) differences among the surfaces, through the time sequence of surveys, and also  
30  
31 460 significant interactions between surfaces and time (Table 1). Canopy height increased  
32  
33 461 significantly from 2005 to 2010 and then to 2013. Furthermore, the canopy was higher at  
34  
35 462 1980EI locations than at 2000PI locations, which was in turn higher than at 2004PI locations,  
36  
37 463 and again higher than at 2000btwn and 2004btwn locations. Significant interactions illustrate  
38  
39 464 how in 2005 all 2000PI and 2004PI surfaces had a low vegetation canopy that was not  
40  
41 465 significantly different from the 2000btwn and 2004btwn locations. However, in later surveys,  
42  
43 466 the canopy progressively increased in height across the 2000PI and 2004PI surfaces, so  
44  
45 467 that the canopy on 2000PI surfaces in 2013 was significantly higher than that on 2000PI  
46  
47 468 surfaces in 2010 and the canopy on 2004PI surfaces in 2013, and these in turn were higher  
48  
49 469 than the canopy on 2004PI surfaces in 2010. The 1980EI surfaces supported the highest  
50  
51 470 vegetation canopy at all dates.  
52  
53  
54 471 The composition of the vegetation was explored in July 2011 and June 2016 through walk-  
55  
56 472 over surveys of 5 pioneer islands of three different ages. Pioneer islands initiated in 2000  
57  
58  
59  
60

and 2004 were explored on both dates as well as newly formed pioneer islands (2010PI in the 2011 survey and 2014PI in the 2016 survey). In addition surveys at five of the 1980EI sampling locations were explored in 2016. Viable seed species were also identified for all 2017 sampled surfaces (1980EI, 2000PI, 2004PI, 2014PI, 2000btwn, 2004btwn, unveg).

In total, 138 plant species were identified across the three surveys. In addition to the earlier survey date, there was a colder spring in 2016 than in 2011. The accumulated growing degree days (GDD) to 18 June 2016, when the vegetation survey commenced, was 470 in comparison with 632 to the same date in 2011, and the accumulated GDD to 22 July 2011, when the vegetation survey commenced in 2011, was 1040. The accumulated solar radiant energy exposure from 1<sup>st</sup> January to 18<sup>th</sup> June 2016 was 1752 MJ/m<sup>2</sup> and from 1<sup>st</sup> January to 18<sup>th</sup> June 2011 was 2339 MJ/m<sup>2</sup> (about 33% more than in 2016 for the same time period). The accumulated solar radiant energy from 1<sup>st</sup> January to 22<sup>nd</sup> July 2011 was 3104 MJ/m<sup>2</sup>. These contrasts in accumulated GDD and solar energy receipt probably explain differences in the standing vegetation. Few species were in flower and many species had probably not emerged sufficiently to be recorded during the June 2016 vegetation survey, whereas vegetation development was much more advanced during the 2011 survey. While 105 species were recorded in the standing vegetation in July 2011, only 76 were recorded in June 2016, and only 30 were recorded in the February 2017 seed bank. Of the 138 recorded species, seven (less than 5%) were alien (*Amorpha fruticosa*, *Aster novi-belgii*, *Buddleja davidii*, *Conyza Canadensis*, *Datura stramonium*, *Juncus tenuis*, *Robinia pseudoacacia*). Of the 30 species identified in the seedbank only two (7%) were alien: *Buddleja davidii* and *Juncus tenuis*. The number of viable seeds in the winter seedbank should also be considered in the light of the stark contrasts in the longevity of the seedbanks associated with the standing vegetation observed across the different types and ages of sampled surfaces described below.

Agglomerative Hierarchical Cluster Analysis was used to explore the similarity in species composition of the standing vegetation (2011, 2016) and the seed bank (2017) (Figure 7).

1  
2  
3 500 The seed bank composition showed very little similarity to the standing vegetation. There  
4  
5 501 was also a contrast in species composition displayed by the two standing vegetation  
6  
7 502 surveys. The species composition of pioneer islands surveyed in 2011 showed reasonable  
8  
9 503 similarity and clustered in turn with the 2000 and 2014 pioneer islands surveyed in June  
10  
11 504 2016. However, the vegetation species composition of 2004 pioneer islands surveyed in  
12  
13 505 2016 was most similar to the 1980 established islands, whereas that of the 2000 pioneer  
14  
15 506 islands surveyed in 2016 was most similar to the 2014 pioneer islands. Furthermore,  
16  
17 507 vegetation composition of the latter was more similar to pioneer islands surveyed in 2011  
18  
19 508 than to the 2016 vegetation of the 2004PI and 1980EI surfaces. This illustrates some notable  
20  
21 509 differences in the rate of development of vegetation on pioneer islands of different date.

22  
23 510 Broad characteristics of the identified species are summarised in Figure 8. Far fewer species  
24  
25 511 were found in the seed bank than in the standing vegetation (Figure 8A). Information on 67%  
26  
27 512 (92) of these species was extracted from Hodgson et al. (1995) and Grime et al. (2007). In a  
28  
29 513 few these cases, where the specific species was not included, it was possible to extract plant  
30  
31 514 strategies and characteristics based on closely related species in the same genus. The  
32  
33 515 number of species according to data source (seed bank, standing vegetation), sampling date  
34  
35 516 and surface type for which characteristics were extracted from Hodgson et al. (1995) is  
36  
37 517 illustrated in Figure 8A (labelled 'species analysed'). Three characteristics of the analysed  
38  
39 518 species - functional type, seed bank type, typical terminal habitat type - are summarised in  
40  
41 519 Figures 8B, C and D, respectively, across the seed bank and standing vegetation data sets  
42  
43 520 for surfaces of different age.

44  
45 521 The February 2017 seed bank was dominated by species whose primary strategy was  
46  
47 522 ruderal, whereas predominantly competitor species were present in the standing vegetation  
48  
49 523 (Figure 8B). Furthermore, the competitor strategy was stronger in species observed on the  
50  
51 524 2004 and 2000 pioneer islands and 1980 established islands than on the early stage pioneer  
52  
53 525 islands (2010 and 2014). Seed bank persistence also varied across the species identified in  
54  
55 526 the seed bank and standing vegetation (Figure 8C), with the seed bank, particularly on



unvegetated bar and between-pioneer island surfaces, being dominated by species associated with a long-term persistent seed bank (i.e. seeds remaining viable for at least five years), whereas the standing vegetation on pioneer and established island surfaces shows an increasing proportion of species associated with a transient seed bank (i.e. seeds that rarely remain viable for more than a year) as the age of the surface increases. The 1980EI surfaces are dominated by species with a transient seed bank (62% species) and a very small proportion (15%) are associated with a long term persistent seed bank.

There are also strong contrasts in the commonest terminal habitat with which the species are associated (Figure 8D). In Figure 8D, the terminal habitats listed in Hodgson et al. (1995) have been aggregated into broad groups related to moisture, vegetation cover and type and degree of natural or human disturbance. The February 2017 seed bank contained a number of species associated with water habitats that were not observed in the standing vegetation, almost no species associated with woodland, none associated with scrub, but species associated with pasture and meadow habitats were present. In contrast, the standing vegetation displayed species whose terminal habitats included pasture and meadow, scrub and woodland, and the proportion of species associated with these terminal habitats increased with surface age. At the same time, although no species associated with water habitats were observed in the standing vegetation, wetland species were present in a declining proportion with surface age and three river bank species were found only in the standing vegetation of pioneer islands. Species associated with bed rock and scree habitats were present in the standing vegetation and seed bank of all investigated surfaces apart from the seedbank samples drawn from unvegetated and between pioneer island surfaces. However, species associated with wasteland habitats were mainly confined to the standing vegetation.

551

## 552 **DISCUSSION**



1  
2  
3  
4  
5  
6  
7  
8  
9  
10  
11  
12  
13  
14  
15  
16  
17  
18  
19  
20  
21  
22  
23  
24  
25  
26  
27  
28  
29  
30  
31  
32  
33  
34  
35  
36  
37  
38  
39  
40  
41  
42  
43  
44  
45  
46  
47  
48  
49  
50  
51  
52  
53  
54  
55  
56  
57

The results presented in this paper support discussion of the evolution of islands over years to decades and also the influential processes that occur over days to months. These themes are discussed below in two subsections, and are followed by a final subsection which includes some concluding remarks and reference to management applications.

**Evolution of islands over years to decades**

Analysis of aerial images (Mardhiah et al., 2015) and field observations confirm that established and pioneer islands that persisted and developed up until the last field campaign in 2017 were initiated by deposition of uprooted trees during flood events that occurred in the mid to late 1970s and during 2000 and 2004 (the last two characterised by a recurrence interval of >10 years and 3 years, respectively). Therefore, pioneer island establishment is not a frequent process. Specific conditions are needed that occur occasionally when compared with the starting processes of vegetation erosion and large wood deposition, which have been observed to occur during low magnitude floods with a recurrence interval in the range 1 to 2.5 years (Bertoldi et al., 2013; Surian et al., 2015). Flood history appears to be more relevant than peak magnitude in island development, as also highlighted by Belletti et al. (2014) in their regional scale study of 12 braided rivers. A combination of morphological reworking, the creation of appropriate surfaces, vegetated bank erosion and deposition of the uprooted trees, followed by a few years of lower flow are all necessary. For example, evidence from airborne Lidar surveys shows a gradual but clear aggradation of the 2004PI surfaces over an 8 year period. Their median detrended elevation increased from - 0.285 m in 2005 to +0.168 m in 2010 to +0.176 m in 2013 (average aggradation of approximately 0.057 m per year). These 2004 pioneer islands were initiated at a very low elevation, compared to that of other uprooted and deposited trees observed in the same reach. Bertoldi et al. (2013) reported trees deposited in the range 0 to 0.5 m during a flood in 2009, and those did not survive subsequent floods. Furthermore, although the 2014 deposited trees could not be located on the 2013 Lidar, it is very likely that they were

deposited at an elevation of approximately 0.1–0.3 m, comparable to that of the 2004 pioneer islands almost 10 years after deposition. A similar wide range of deposited tree elevation was reported also by Räßle et al., 2017 (when transformed from elevation above low flow to elevation above the mean). This reinforces the crucial role played by flood history. The survival of the 2004 pioneer islands was possible only because of the occurrence of 3 particularly dry years following their deposition, enabling deposited trees to anchor themselves and grow before being affected by significant flood disturbance.

The evidence for aggradation of the older and higher 2000PI and 1980EI surfaces over this period is equivocal, suggesting a rapid slowing in aggradation once island surfaces have developed above the level of relatively frequent inundation (e.g. elevations that are reached for less than one day per year, Figure 3).

The islands developed around deposited uprooted trees and aggraded as new trees sprouted from them (e.g. Figure 1, 2002 image shows sprouting trees deposited in 2000). In nearly all cases, the deposited trees that initiate pioneer islands in the study reach are black poplar (*Populus nigra*), a facultative phreatophyte capable of rapid root growth in response to different water and sediment conditions (Holloway et al., 2017a, b, c), and the Lidar data and field measurements show that deposited trees of this species can regenerate to produce a canopy that grows rapidly, particularly in the first 15 years following deposition (Figure 6A). The median canopy height increased from 0.24 to 6.85 m (6.61 m growth) on the 2004PI surfaces, from 1.64 to 9.76 m (8.72 m growth) on the 2000PI surfaces and from 22.79 to 25.04 m (2.83 m growth) on the 1980EI surfaces between 2005 and 2013. These data suggest that after the first couple of years following deposition, an annual growth increment of over 1 m per year above the aggrading island surface is achieved in the study reach over at least a 15 year period. Since the growth develops from a deposited tree, which then becomes buried, the actual annual growth rate from the elevation at which the tree was deposited is slightly greater than this in these early years.

1  
2  
3 606 As islands aggrade, they also extend laterally through aggradation and coalescence. This  
4  
5 607 lateral aggradation can be clearly seen in the vegetated area surrounding the studied 2000  
6  
7 608 and 2004 pioneer islands in Figure 1 (compare the 2002 and 2015 images at the sampling  
8  
9 609 locations), and is supported by increases in vegetation canopy height and emergence of a  
10  
11 610 vegetation canopy between pioneer islands (Figure 6A). The annual growth rate of trees on  
12  
13 611 the 2000 and 2004 pioneer islands is quite constant when measured on a time scale of 3 to  
14  
15 612 5 years, with no apparent marked changes between particular years (Figure 6A). The time  
16  
17 613 scale is probably long enough to filter out the impact of annual changes in temperature and  
18  
19 614 precipitation, masking the controls highlighted by Raple et al., 2017. More importantly, once  
20  
21 615 the trees have survived initial deposition and early establishment, which is affected by  
22  
23 616 access to groundwater and thus river stage (e.g. Francis, 2007), there seems to be a  
24  
25 617 negligible impact of local bed elevation on their rate of growth. This comparable growth rate  
26  
27 618 regardless of elevation indicates high water availability in the study reach, which is mainly  
28  
29 619 characterised by groundwater upwelling (Doering et al., 2007). On other reaches of the  
30  
31 620 Tagliamento, such a constant rate of growth may not occur, since there are notable  
32  
33 621 differences between reaches (Gurnell, 2016) that highlight sensitivity to changes in moisture  
34  
35 622 availability, and such sensitivity to relative elevation with respect to groundwater may be an  
36  
37 623 important factor in island development across other river environments.  
38  
39 624 As sediments accumulate around the growing *P.nigra* trees, their properties change (Figure  
40  
41 625 4). While unvegetated bar surfaces are characterised by gravel deposits, higher surfaces  
42  
43 626 show increasingly fine deposits. Well-vegetated island surfaces (1980EI, 2000PI and  
44  
45 627 2004PI) show predominantly sandy surface sediments containing varying amounts of silt,  
46  
47 628 clay and organic material, whereas sparsely-vegetated surfaces of the youngest pioneer  
48  
49 629 islands (2014PI) and areas between the older pioneer islands (2000btwn, 2004btwn) show  
50  
51 630 coarser gravel-sand mixtures (Figure 4). Thus sediments fine with increasing elevation and  
52  
53 631 vegetation cover, presumably because finer sediments on sparsely-vegetated elevated  
54  
55 632 surfaces between pioneer islands are subject to flow funnelling and higher shear stresses  
56  
57  
58  
59  
60

633 during major inundating flood events that may mobilise finer sediments. The role of fine  
634 sediments is relevant for island development, but not crucial for island initiation. Deposited  
635 trees are able to trap fine sediments soon after they sprout and grow branches and leaves.  
636 For example, after less than 2 years and a few moderate floods, the grain size distribution of  
637 the 2014PI surfaces show a clear fining. The subsequent growth of shrubs and then herbs  
638 and grasses forms a vegetated surface that is increasingly efficient at trapping fine  
639 sediments and organic matter as islands age.

640 The number of plant species and the vegetation composition of islands also changes with  
641 increasing age (Figure 8). Focussing on the vegetation survey conducted in 2011 and  
642 following a warm spring, the number of species in the standing vegetation increases steadily  
643 from 1 year old (2010PI) through seven year old (2004PI) to 11 year old (2000PI) islands as  
644 new species progressively colonise the developing island surfaces (Figure 8A). The 2016  
645 vegetation survey, following a cool spring, recorded fewer species than the 2011 survey,  
646 with little difference in the number of species on two year (2014PI) and 12 year (2004PI)  
647 pioneer islands. The largest number of species were observed on 16 year old pioneer  
648 islands (2000PI), with established islands (1980EI) showing less species than all of the  
649 pioneer islands (Figure 8A). This suggests that as islands aggrade, new species appear until  
650 the tree canopy closes and the trees and shrubs out-compete many other species, following  
651 typical seral trajectories wherein species are excluded by dominant competitors and diversity  
652 peaks in the mid-seral stages; though this trend is also likely to be an expression of the  
653 intermediate disturbance hypothesis (Connell, 1978; Tabacchi et al., 1998; Bendix and  
654 Hupp, 2000) whereby the largest number of species are supported on surfaces subject to an  
655 intermediate level of flood disturbance. However, the reduction in species present on  
656 established island surfaces is likely to be counteracted by species colonising areas of wood  
657 and sediment deposition, sprouting and aggradation at and near island edges that create  
658 new local island-margin patches, particularly at the sheltered downstream island tail, that  
659 may emulate the vegetation development processes observed on pioneer islands.

1  
2  
3  
4  
5  
6  
7  
8  
9  
10  
11  
12  
13  
14  
15  
16  
17  
18  
19  
20  
21  
22  
23  
24  
25  
26  
27  
28  
29  
30  
31  
32  
33  
34  
35  
36  
37  
38  
39  
40  
41  
42  
43  
44  
45  
46  
47  
48  
49  
50  
51  
52  
53  
54  
55  
56  
57  
58  
59  
60

The supposition concerning canopy closure and competition is also supported by the average C, S and R scores of the species that are present. With increasing surface age, the vegetation becomes increasingly dominated by competitor species, whereas the youngest pioneer islands show a balance of competitor, stress-tolerator and ruderal species (Figure 8B). Furthermore, the proportion of species associated with wetland, arable, wasteland and bedrock terminal habitats decreases and the proportion with woodland and scrub terminal habitats increases with surface age (Figure 8D), as a more stable ‘climax’ riparian woodland emerges. The change in vegetation cover, height and composition with increasing island age is accompanied by an increase in the organic content, roots and fungal hyphae as the fining surface sediments start to develop into soils with increasing island age (Figure 6). These observations support the island development model proposed by Gurnell et al. (2001) and provide considerable detail on the functioning of that model over annual to decadal timescale.

**Influential processes over days to months**

Large flood events are crucial to the island model, and so it is unsurprising that the largest flood in the period 2000 to 2017 (on 5<sup>th</sup> November 2000, Figure 2) was responsible for initiating numerous, widely distributed pioneer islands in the study reach. The flood event in 2004 (on 31<sup>st</sup> October, Figure 2) was more localised than the 2000 event with trees released by erosion of the floodplain around a tributary being deposited across a relatively small area of the river bed (Francis et al., 2008). However, the resulting pioneer islands have grown rapidly to the present, despite the occurrence of a larger flood in 2012 (on 12<sup>th</sup> November, Figure 2). This survival can probably be attributed to a four year period without significant floods following the 2004 event, which allowed these 2004 pioneer islands to establish and aggrade sufficiently to resist erosion. The occurrence of the large flood in 2012 may also explain why trees deposited by smaller flood peaks on 30<sup>th</sup> October 2008, 25<sup>th</sup> December

2009 and 1<sup>st</sup> November 2010 (Figure 2) have not developed into longer-term pioneer islands. However, it will be interesting to observe whether any of the 2014 pioneer islands (deposited on 6<sup>th</sup> November) are able to survive in the longer term, given the relatively low flows since their deposition (Figure 2).

Information gained from the field campaigns in 2016 and 2017 provides indications of the potential importance of several processes in island development. Between these two field campaigns, there were three small flood events on 14<sup>th</sup> July, 6<sup>th</sup> and 19<sup>th</sup> November 2016 (Figure 9), with a maximum water elevation of 0.25m (detrended elevation) on 14<sup>th</sup> July 2016. This maximum elevation would have inundated all unvegetated surfaces and most of the 2014PI, 2004PI and 2004btwn surfaces (Figure 3). The vegetation cover on the latter three surfaces (2014PI, 2004PI, 2004btwn) is likely to have retained sediment from these floods as they receded, and since the floods are relatively small, the transported sediment is likely to have been quite fine, partly explaining the sediment fining on these surfaces between the two sampling campaigns (Figure 5). However, these flood events cannot explain sediment fining on higher surfaces. Gurnell et al. (2008) proposed wind storms as being another important mechanism for transporting sediments along the Tagliamento river corridor that can be intercepted and deposited on vegetated surfaces. This proposal was founded on a unique sequence of events which resulted in the production of very fine surface crusts, whose properties suggested wind as the most likely transporting agent. Wind storms transporting dense dust particles are quite common on the Tagliamento and their importance may be underestimated on other braided rivers where vast areas of exposed sediments can provide fine sediment for wind transport. Between field campaigns, there was a wind speed maximum of 26.3 m/s on 13 July and a period from 8<sup>th</sup> to 12<sup>th</sup> November 2016 when daily maximum wind speeds exceeded 15 m/s, with a maximum of 23.1 m/s on 10<sup>th</sup> November 2016. Moreover, almost no precipitation occurred in December 2016 and January 2017, whereas several days had a maximum wind speed larger than 10 m/s, suggesting dry conditions may have favoured wind transport. Wind transport may explain the deposition of

finer sediments on surfaces that were not inundated between the field campaigns, particularly as the wind-deposited crusts sampled by Gurnell et al. (2008) within the study reach had an average D90 grain size of 6.7  $\phi$ , which compares favourably with the increases in D90 illustrated in Figure 5. These observations suggest that wind as well as water may play a role in the aggradation and fining of surface sediments as islands increase in age and surface elevation on the Tagliamento and possibly other braided rivers.

Finally, the winter seed bank data has some relevance for both short and long term processes of island development. It is unsurprising that there is low similarity between the species in the seedbank and established vegetation (Figure 7) as a lack of similarity has been observed in the riparian seed bank and standing vegetation of other river systems, which have also shown a high seasonal variability in seed bank composition (e.g. Gurnell et al., 2006, 2008). However, the lack of similarity between the winter seedbank and vegetation composition in the present study is particularly stark. Since the seed bank was sampled in winter, it is not surprising that it mainly contained species that are associated with a persistent seed bank (Figure 8C). However, there is evidence that at least some of the seed species that were sampled have been transported into the sampling locations. In particular, some aquatic species are present in the seed bank but not in the standing vegetation. Whilst this is not surprising given their habitat requirements (there are no water bodies on the islands and aquatic species are rarely found in the ponds adjacent to pioneer and established islands), their presence illustrates that they have been dispersed into the sampled surface sediments. Their most likely source is a tributary stream that enters the Tagliamento main stem at the upstream end of the study reach and supports a variety of aquatic plant species, or they may have arrived from other upstream water bodies. Although water transport may explain the presence of these seed species on the 2004PI and 2004btwn surfaces, their presence on higher surfaces (Figure 8D) cannot be explained by water transport but could be explained by remobilisation and deposition by wind. Both wind and water are recognised as important means of seed dispersal (Fenner and Thompson,



2005) and both are likely to be associated with deposition of seeds on island surfaces by events that occur over periods of hours to days, transporting seeds from their source areas and also remobilising them from other parts of the river bed and margins. In addition, larger vegetative propagules may be transported and deposited by floods to add to living plants and propagules co-deposited with soils attached to uprooted, deposited trees. One final point that relates to both dispersal mechanisms and aggradation, is that the 2004 islands stand out as not only having the highest decadal aggradation rates (Figure 3); the highest seed abundance (Figure 6) and highest number of species (Figure 8A) in their seedbank; and a remarkable development in their standing vegetation (Figures 7 and 8); but in the short term (between 2016 and 2017 sampling) they were affected by both wind and water dispersal processes (Figure 9), enabling enhanced sediment delivery, surface aggradation and the delivery and retention of plant propagules from a wide variety of locations and thus a potentially substantial species pool. Such fine-scale patterns of propagule deposition and plant colonisation are likely to add to the complexity of island development and contribute to the shifting habitat mosaic found at multiple scales within the Tagliamento's island-braided reaches (e.g. Ward et al., 2002a).

### Management Applications and Concluding Remarks

The recognition of islands as important landscape elements that are indicative of river ecosystem function and health (Tockner et al., 2003; Beechie et al., 2006) has led to increased interest in incorporating such landforms and their underlying processes into river restoration and management efforts. For example, Wyrick and Klingeman (2011) note that despite their widespread occurrence and ecological importance, islands are rarely incorporated into river restoration concepts. They propose a process-based island classification scheme that can identify island types, their formative processes and the relationship between island formation and river processes in general. As Wyrick and Klingeman (2011) indicate, any incorporation of islands and island-building processes in



1  
2  
3 767 river restoration and management need to be cognizant of both the mechanisms and  
4  
5 768 timescales of development that we have begun to explore here. In particular, our data and  
6  
7 769 similar measurements from other river systems can contribute to the refinement and testing  
8  
9 770 of numerical models that are increasingly incorporating physically based  
10  
11 771 vegetation/morphology feedbacks and could provide important means of forecasting likely  
12  
13 772 evolutionary trajectories of vegetated landforms under different environmental conditions  
14  
15 773 (e.g. van Oorschot et al., 2016; Zen et al., 2016).  
16  
17 774 Gurnell et al. (2001, updated 2012, 2016) presented a conceptual model of island  
18  
19 775 development based on observations along the braided, gravel-bed Tagliamento River. Since  
20  
21 776 then, the expanding literature on river island development, has primarily focused on the  
22  
23 777 formative physical processes of island development, their morphological evolution,  
24  
25 778 sedimentary environments, or aspects of their ecology and biodiversity (e.g. Mikuš et al.  
26  
27 779 2013; Picco et al. 2015; Raška et al. 2016; Vanbergen et al., 2017). In this paper we have  
28  
29 780 integrated these different perspectives and considered them across different timescales.  
30  
31 781 Although the datasets are not as comprehensive as we would like, this is often the case with  
32  
33 782 ecological data in complex and dynamic ecosystems, but we nevertheless consider them  
34  
35 783 sufficient to provide valuable information on elements of island development where  
36  
37 784 knowledge is notably sparse.  
38  
39  
40 785 First, we have provided support to the view that when islands are initiated by the sprouting of  
41  
42 786 deposited trees (the ‘regeneration from living wood’ pathway; Gurnell et al., 2001), the  
43  
44 787 elevation of the tree deposition site matters (see also Francis, 2007). Trees are only  
45  
46 788 uprooted, transported and deposited in sizeable numbers during relatively large flood events  
47  
48 789 (e.g. Comiti et al., 2016), with deposition occurring during the peak and falling limb of these  
49  
50 790 flood events (e.g. MacVicar et al., 2009). Depositionary location governs both water access  
51  
52 791 (the lower the elevation, the closer to the water table) and likelihood of disturbance and  
53  
54 792 removal prior to establishment (the higher the elevation, the less likely they will be  
55  
56 793 disturbed). Therefore, if trees are deposited at low elevation, where they have access to

794 water to support rapid growth, river flows in the first two to three years following deposition  
795 are critical to their survival. If no major floods occur in this early period after deposition the  
796 trees can develop significant root and shoot biomass to anchor them and enable them to  
797 trap transported sediments, increase their surface elevation and thus reduce the level of flow  
798 disturbance to which they are subsequently subjected. These early developmental  
799 processes and timeframes are likely to be applicable to all island braided rivers where island  
800 development is initiated by sprouting of uprooted trees, and highlight the importance of  
801 regenerating trees having sufficient access to water and limited fluvial disturbance during  
802 initial years of establishment if island formation is to be facilitated.

803 Second, we have shown that once early establishment has occurred, islands aggrade their  
804 surfaces and develop a vegetation canopy at a remarkably steady rate over a decadal time  
805 scale. As islands aggrade and above-ground vegetation biomass and canopy height  
806 increase, there is also a steady fining of surface sediments and an increase in their organic  
807 content, including living material such as roots and fungal hyphae. This steady development  
808 reflects the fact that the study reach is subject to groundwater upwelling and thus possesses  
809 a fairly consistent and reliable moisture supply to support growth of the main tree species  
810 driving island initiation and development along the Tagliamento: *Populus nigra*. Thus, in the  
811 case of the study reach, *P. nigra* acts as a true ecosystem engineer (Jones et al., 1994,  
812 Gurnell, 2014), and our observations are likely to be applicable to other river reaches where  
813 water table fluctuations operate within a relatively small range and where *Populus nigra* or  
814 other riparian Salicaceae that are similarly sensitive to moisture availability and groundwater  
815 depth are driving pioneer island development. In reaches where major water table  
816 fluctuations occur, survival of deposited trees will be more sensitive to the elevation at which  
817 they are deposited, as will their subsequent rate of establishment. The initial establishment  
818 and growth of islands and the development of their surface sediments and vegetation cover  
819 as well as their ability to withstand subsequent flood events will vary not only with the river  
820 flow regime but also with the groundwater regime (e.g. Bätz et al., 2016) and any

1  
2  
3 821 confounding climatic trends (low rainfall, high evaporation). Detailed analyses to compare  
4  
5 822 island and associated dynamics in reaches subject to different groundwater / water  
6  
7 823 availability conditions are needed to more fully investigate the integrated biological and  
8  
9 824 geomorphological implications for island evolution, and how this may relate to management  
10  
11 825 and restoration.  
12  
13 826 Third, we found the maximum number of plant species, seed bank species, and seed  
14  
15 827 abundance to be associated with island surfaces of intermediate age and elevation,  
16  
17 828 reflecting seral trajectories and patterns of disturbance. This further highlights the  
18  
19 829 importance of allogenic disturbances and complex dynamics that shape the ecology of  
20  
21 830 building islands, which may serve to confound easy prediction of, for example, plant  
22  
23 831 community development. In an early study, Nagel et al. (1980) observed that river islands  
24  
25 832 along the lower energy, regulated Platt River in Nebraska (USA) presented similar trends of  
26  
27 833 soil development and aggradation with island age, but also that although plant diversity and  
28  
29 834 abundance of perennials increased with island age, island communities remained broadly  
30  
31 835 similar and at early seral stages. Expectations around ecological development and  
32  
33 836 succession of river islands, for example if used an indicators of ecosystem health or in  
34  
35 837 restoration efforts, should therefore take into account the complexity of factors determining  
36  
37 838 assemblages, which will vary between reaches and river systems. In our case for example,  
38  
39 839 islands of intermediate age had a rather particular initiation and evolution history, and more  
40  
41 840 work would be needed to establish the transferability of our findings to other contexts.  
42  
43  
44 841 Finally, our most speculative finding relates to the importance of climatic conditions in  
45  
46 842 influencing island evolution at event to seasonal timescales. We have observed significant  
47  
48 843 fining of surface sediments on all vegetated surfaces over a period of approximately six  
49  
50 844 months. Whereas some of this fining can be attributed to deposition of fine sediments  
51  
52 845 transported by small flood events on inundated vegetated surfaces, many of the surfaces  
53  
54 846 showing fining were not inundated. Based on earlier observations (Gurnell et al., 2008), we  
55  
56 847 have suggested wind as a potentially important agent for transporting fine sediments that

become trapped by vegetation, particularly during dry periods. Aeolian fine sediments and dusts (including organic particulates) have been found to be more pervasive and ecologically important in ecosystems than usually assumed, for example contributing to river nutrient loads, especially in more arid basins (e.g. McTainsh and Strong 2007). McGowan et al. (1996) note that dust entrainment may be particularly prevalent along alpine river valleys, where the topography can channel high wind speeds. On the study reach and higher up the river, fine deposits on exposed bars, especially at high elevations, may represent a source of fine sediments that become trapped by vegetation. Wind is also recognised as a major agent for seed transport; most notably in the present context for the transport of the abundant short-lived seeds of the Salicaceae, alongside and in combination with water (e.g. Boland 2014, 2017). Wind may therefore have agency in island aggradation and also the delivery of seeds from terrestrial and riparian species pools, though further work is needed to confirm this. Furthermore, we have provided some support for a potentially important role of temperature conditions in the annual cycle of vegetation development and flowering. Species which only show above-ground biomass seasonally could be an important influence on seasonal fine sediment trapping and retention of surface moisture through the late spring and summer months. Thus, while flood and low flow events are clearly the key controls on island evolution, various climatic variables may be extremely important for fine sediment retention, soil development and other short term facets of island evolution, and should be considered in any management or restoration context. However, more research is needed to verify and quantify these influences

869

## 870 **ACKNOWLEDGMENTS**

871 Figure 1 includes two images from Google Earth, both from the same supplier: Image ©  
872 2017 DigitalGlobe. In using these images, we have conformed to guidelines available from  
873 <http://www.google.com/permissions/geoguidelines/attr-guide.html> (accessed 16 December  
874 2017) including image attributions in the Figure caption that conform to 'the text of your

1  
2  
3 875 attribution must say the name “Google” and the relevant data provider(s), such as “Map  
4  
5 876 data: Google, DigitalGlobe” and we have not obtained written permission to use these  
6  
7 877 images because the guidelines state that ‘Due to limited resources and high demand, we’re  
8  
9 878 unable to sign any letter or contract specifying that your project or use has our explicit  
10  
11 879 permission’. The authors acknowledge the UK Natural Environment Research Council for  
12  
13 880 providing the 2005 lidar data; Nicola Surian, University of Padova (CARIPARO project) for  
14  
15 881 the 2010 lidar data and Yasuhiro Takemon, University of Kyoto for the 2013 lidar data. Ulfah  
16  
17 882 Mardhiah’s research was funded by the SMART Joint Doctoral Programme (Science for  
18  
19 883 MAnagement of Rivers and their Tidal systems), which is financed by the Erasmus Mundus  
20  
21 884 Programme of the European Union. We thank C. Cruciat, S. Arcandi, M. Benvegnù and M.  
22  
23 885 Welber for helping during the field data collection.

24 886  
25  
26 887

28 888 **REFERENCES**

31 889 Bätz N, Colombini P, Cherubini P, Lane SN. 2016. Groundwater controls on biogeomorphic  
32  
33 890 succession and river channel morphodynamics. *Journal of Geophysical Research: Earth*  
34  
35 891 *Surface*, 21(10): 1763-1785.  
36  
37  
38 892 Bätz N, Verrecchia EP, Lane SN. 2015. The role of soil in vegetated gravelly river braid  
39  
40 893 plains: more than just a passive response? *Earth Surface Processes and Landforms*, 40(2):  
41  
42 894 143-156.  
43  
44 895 Baubinienė A, Satkūnas J, Taminskas J. 2015. Formation of fluvial islands and its  
45  
46 896 determining factors, case study of the River Neris, the Baltic Sea basin. *Geomorphology*,  
47  
48 897 231(Supplement C): 343-352.  
49  
50  
51 898 Belletti B, Dufour S, Piégay H. 2014. Regional assessment of multidecadal changes in  
52  
53 899 braided riverscapes following large floods (example of 12 reaches in south east of France).  
54  
55 900 *Advances in Geosciences*, 37: 57-71

- 901 Belletti B, Dufour S, Piégay H. 2015. What is the relative effect of space and time to explain  
902 the braided river width and island patterns at a regional scale? *River Research and*  
903 *Applications*, 31(1): 1-15.
- 904 Bendix J, Hupp CR. 2000. Hydrological and geomorphological impacts on riparian plant  
905 communities. *Geomorphology*, 14: 2977-2990.
- 906 Bertoldi W, Gurnell AM, Drake NA. 2011. The topographic signature of vegetation  
907 development along a braided river: results of a combined analysis of airborne lidar, colour air  
908 photographs and ground measurements. *Water Resources Research*, 47: W06525, 13pp.
- 909 Bertoldi W, Gurnell AM, Surian N, Tockner K, Zanoni L, Ziliani L, Zolezzi G. 2009.  
910 Understanding reference processes: linkages between river flows, sediment dynamics and  
911 vegetated landforms along the Tagliamento River, Italy. *River Research and Applications*,  
912 25: 501-516.
- 913 Bertoldi W, Gurnell AM, Welber M. 2013. Wood recruitment and retention: The fate of  
914 eroded trees on a braided river explored using a combination of field and remotely-sensed  
915 data sources. *Geomorphology*, 180-181(1): 146-155.
- 916 Bertoldi W, Welber M, Gurnell AM, Mao L, Comiti F, Tal M., 2015. Physical modelling of the  
917 combined effect of vegetation and wood on river morphology. *Geomorphology*, 246: 178-  
918 187.
- 919 Blott SJ, Pye K. 2001. GRADISTAT: a grain size distribution and statistics package for the  
920 analysis of unconsolidated sediments. *Earth Surface Processes and Landforms*, 26: 1237-  
921 1248.
- 922 Bollati I, Pellegrini L, Rinaldi M, Duci G, Pelfini M. 2014. Reach-scale morphological  
923 adjustments and stages of channel evolution: The case of the Trebbia River (northern Italy).  
924 *Geomorphology*, 221: 176-186.

- 925 Bywater-Reyes S, Wilcox AC, Diehl RM. 2017. Multiscale influence of woody riparian  
926 vegetation on fluvial topography quantified with ground-based and airborne lidar. *Journal of*  
927 *Geophysical Research: Earth Surface*, 122(6): 2016JF004058.
- 928 Connell JH. 1978. Diversity in tropical rain forests and coral reefs. *Science*, 199(4335):  
929 1302-1310.
- 930 Corenblit D, Steiger J, Charrier G, Darrozes J, Garófano-Gómez V, Garreau A, González E,  
931 Gurnell AM, Hortobágyi B, Julien F, Lambs L, Larrue S, Otto T, Roussel E, Vautier F,  
932 Voltaire O. 2016. *Populus nigra* L. establishment and fluvial landform construction:  
933 biogeomorphic dynamics within a channelized river. *Earth Surface Processes and*  
934 *Landforms*, 41(9): 1276-1292.
- 935 Corenblit D, Steiger J, Gurnell AM, Tabacchi E, Roques L. 2009. Control of sediment  
936 dynamics by vegetation as a key function driving biogeomorphic succession within fluvial  
937 corridors. *Earth Surface Processes and Landforms*, 34(13): 1790-1810.
- 938 Diehl RM, Wilcox AC, Stella JC, Kui L, Sklar LS, Lightbody A. 2017. Fluvial sediment supply  
939 and pioneer woody seedlings as a control on bar-surface topography. *Earth Surface*  
940 *Processes and Landforms*, 42(5): 724-734.
- 941 Doering M, Uehlinger U, Rotach A, Schlaepfer DR, Tockner K. 2007. Ecosystem expansion  
942 and contraction dynamics along a large Alpine alluvial corridor (Tagliamento River,  
943 Northeast Italy). *Earth Surface Processes and Landforms*, 32: 1693-1704
- 944 Fenner M, Thompson K. 2005. *The ecology of seeds*. Cambridge University Press,  
945 Cambridge, 250pp.
- 946 Francis RA. 2007. Size and position matter: riparian plant establishment from fluvially  
947 deposited trees. *Earth Surface Processes and Landforms*, 32: 1239-1243.



- Francis R, Gurnell AM. 2006. Initial establishment of vegetative fragments within the active zone of a braided gravel-bed river (River Tagliamento, NE Italy). *Wetlands Ecology and Management*, 26(3): 641-648.
- Francis R, Gurnell AM, Petts GE, Edwards PJ. 2005. Survival and growth response of *Populus nigra*, *Salix elaeagnos* and *Alnus incana* cuttings to varying levels of hydric stress. *Forest Ecology and Management*, 210(1-3): 291-301.
- Francis R, Gurnell AM, Petts GE, Edwards PJ. 2006. Riparian tree establishment on gravel bars: interactions between plant growth strategy and the physical environment. In: Sambrook Smith GH, Best JL, Bristow CS, Petts GE. (Editors). *Braided Rivers: Process, Deposits, Ecology and Management*. Blackwell, Oxford, UK, pp. 361-380.
- Francis RA, Tibaldeschi P, McDougall L. 2008. Fluvially-deposited large wood and riparian plant diversity. *Wetlands Ecology and Management*, 16(5): 371-382.
- Gran KB, Tal M, Wartman ED. 2015. Co-evolution of riparian vegetation and channel dynamics in an aggrading braided river system, Mount Pinatubo, Philippines. *Earth Surface Processes and Landforms*, 40(8): 1101-1115.
- Grime JP, Hodgson JG, Hunt R. 2007. *Comparative plant ecology: a functional approach to common British species*, 2<sup>nd</sup> edition, Castlepoint Press, Dalbeattie, UK, 748p.
- Gurnell AM. 2014. Plants as river system engineers. *Earth Surface Processes and Landforms*, 39: 4-25.
- Gurnell AM. 2016. Trees, wood and river morphodynamics: results from 15 years research on the Tagliamento River, Italy. In: Gilvear D, Greenwood M, Thoms M, Wood P. (Editors). *River Systems: Research and Management for the 21st Century*. Wiley, pp. 132-155.
- Gurnell AM, Bertoldi W, Corenblit D. 2012. Changing river channels: the roles of hydrological processes, plants and pioneer landforms in humid temperate, mixed load, gravel bed rivers. *Earth Science Reviews*, 111: 129-141.



- 973 Gurnell AM, Boitsidis AJ, Thompson K, Clifford NJ. 2006. Seed bank, seed dispersal and  
974 vegetation cover: Colonization along a newly-created river channel. *Journal of Vegetation*  
975 *Science*, 17: 665-674.
- 976 Gurnell AM, Blackall TD, Petts GE. 2008. Characteristics of freshly deposited sand and finer  
977 sediments along an island-braided, gravel-bed river: The roles of water, wind and trees.  
978 *Geomorphology*, 99: 254-269.
- 979 Gurnell AM, Petts GE. 2002. Island-dominated landscapes of large floodplain rivers, a  
980 European perspective. *Freshwater Biology*, 47: 581-600.
- 981 Gurnell AM, Corenblit D, García de Jalón D, González del Tánago M, Grabowski RC,  
982 O'Hare MT, Szewczyk M. 2011. A conceptual model of vegetation-hydrogeomorphology  
983 interactions within river corridors. *River Research and Applications*, 32: 142-163.
- 984 Gurnell AM, Petts GE, Hannah DM, Smith BPG, Edwards PJ, Kollmann J, Ward JV, Tockner  
985 K. 2001. Riparian vegetation and island formation along the gravel-bed Fiume Tagliamento,  
986 Italy. *Earth Surface Processes and Landforms*, 26(1): 31-62.
- 987 Gurnell AM, Thompson K, Goodson J, Moggridge H. 2008. Propagule deposition along river  
988 margins: linking hydrology and ecology. *Journal of Ecology*, 96: 553–565.
- 989 Gurnell A, Tockner K, Edwards PJ, Petts GE. 2005. Effects of deposited wood on  
990 biocomplexity of river corridors. *Frontiers in Ecology and Environment*, 3(7): 377–382.
- 991 Hodgson JG, Grime JP, Hunt R, Thompson K. 1995. The electronic comparative plant  
992 ecology, Chapman and Hall, London, UK, 19p.
- 993 Holloway JV, Rillig MC, Gurnell AM. 2017a. Physical environmental controls on riparian root  
994 profiles associated with black poplar (*Populus nigra* L.) along the Tagliamento River, Italy.  
995 *Earth Surface Processes and Landforms*, 42: 1262-1273.
- 996 Holloway JV, Rillig MC, Gurnell AM. 2017b. Underground Riparian Wood: Buried Stem and  
997 Coarse Root Structures of Black Poplar (*Populus nigra* L.). *Geomorphology*, 279: 188-198.

- 998 Holloway JV, Rillig MC, Gurnell AM. 2017c. Underground Riparian Wood: Reconstructing  
999 the processes influencing buried stem and coarse root structures of Black Poplar (*Populus*  
1000 *nigra* L.). *Geomorphology*, 279: 199-208.
- 1001 Hunt R, Hodgson JG, Thompson K, Bungener P, Dunnett NP, Askew AP. 2004. A new  
1002 practical tool for deriving a functional signature for herbaceous vegetation, *Applied*  
1003 *Vegetation Science*, 7: 163-170.
- 1004 Hupp CR, Osterkamp WR. 1996. Riparian vegetation and fluvial geomorphic processes.  
1005 *Geomorphology*, 14: 277-295.
- 1006 Jones CG, Lawton JH, Shachak M. 1994. Organisms as ecosystem engineers. *Oikos* 69:  
1007 373–386.
- 1008 Mardhiah U, Caruso T, Gurnell AM, Rillig MC. 2014. Just a matter of time: Fungi and roots  
1009 significantly and rapidly aggregate soil over four decades along the Tagliamento River, NE  
1010 Italy. *Soil Biology and Biochemistry*, 75: 133-142.
- 1011 Mardhiah U, Rillig MC, Gurnell AM. 2015. Reconstructing the development of sampled sites  
1012 on fluvial island surfaces of the Tagliamento River, Italy, from historical sources. *Earth*  
1013 *Surface Processes and Landforms*, 40(5): 629-641.
- 1014 Moggridge H, Gurnell AM. 2009. Controls on the sexual and asexual regeneration of  
1015 *Salicaceae* along a highly dynamic, braided river system. *Aquatic Sciences*, 71: 305-317.
- 1016 Moretto J, Rigon E, Mao L, Picco L, Delai F, Lenzi MA. 2014. Channel adjustments and  
1017 island dynamics in the Brenta river (Italy) over the last 30 years. *River Research and*  
1018 *Applications*, 30(6): 719-732.
- 1019 Osterkamp WR. 1998. Processes of fluvial island formation, with examples from Plum  
1020 Creek, Colorado and Snake River, Idaho. *Wetlands*, 18(4): 530-545.

1  
2  
3 1021 Osterkamp WR, Johnson WC, Dixon M.D. 2001. Biophysical gradients related to channel  
4  
5 1022 islands, middle Snake River, Idaho. In: Dorava J, Palcsak B, Fitzpatrick F, Montgomery D.  
6  
7 1023 (Editors). Geomorphic Processes and Riverine Habitat. American Geophysical Union,  
8  
9 1024 Washington, D.C., pp. 73-83.  
10  
11 1025 Perona P, Crouzy B, McLelland S, Molnar P, Camporeale C. 2014. Ecomorphodynamics of  
12  
13 1026 rivers with converging boundaries, *Earth Surface Processes and Landforms*, 39: 1651-1662  
14  
15  
16 1027 Räßle B, Piégay H, Stella JC, Mercier D. 2017. What drives riparian vegetation  
17  
18 1028 encroachment in braided river channels at patch to reach scales? Insights from annual  
19  
20 1029 airborne surveys (Drôme River, SE France, 2005–2011). *Ecohydrology*, 10(8): e1886.  
21  
22  
23 1030 Schnauder I, Moggridge HL. 2009. Vegetation and hydraulic-morphological interactions at  
24  
25 1031 the individual plant, patch and channel scale. *Aquatic Sciences*, 71: 318.  
26  
27 1032 Surian N, Barban M, Ziliani L, Monegato G, Bertoldi W, Comiti F. 2015. Vegetation turnover  
28  
29 1033 in a braided river: frequency and effectiveness of floods of different magnitude. *Earth*  
30  
31 1034 *Surface Processes and Landforms*, 40: 542-558.  
32  
33  
34 1035 Tabacchi E, Correll DL, Hauer R, Pinay G, Planty-Tabacchi A-M, Wissmar RC. 1998.  
35  
36 1036 Development, maintenance and role of riparian vegetation in the river landscape. *Freshwater*  
37  
38 1037 *Biology*, 40: 497-516.  
39  
40 1038 Thompson K, Bakker JP, Bekker RM. 1997. The soil seed banks of North West Europe.  
41  
42 1039 Cambridge University Press, Cambridge, 276pp.  
43  
44  
45 1040 Van Oorschot M, Kleinans MG, Geerling GW, Middlekoop H. 2016. Distinct patterns of  
46  
47 1041 interaction between vegetation and morphodynamics. *Earth surface processes and*  
48  
49 1042 *Landforms*, 41: 791-808.  
50  
51 1043 Ward JV, Malard F, Tockner K. 2002a. Landscape ecology: a framework for integrating  
52  
53 1044 pattern and process in river corridors. *Landscape Ecology*, 17: 35-45.  
54  
55  
56  
57  
58  
59  
60

- 1045 Ward JV, Tockner K, Arscott DB, Claret C. 2002b. Riverine landscape diversity. *Freshwater*  
 1046 *Biology*, 47: 517-539.
- 1047 Welber M, Bertoldi W, Tubino M. 2012. The response of braided planform configuration to  
 1048 flow variations, bed reworking and vegetation: the case of the Tagliamento River, Italy. *Earth*  
 1049 *Surface Processes and Landforms*, 37: 572-582.
- 1050 Wetzel PR. 2002. Tree island ecosystems of the World. In: F.H. Sklar and A.G. van der Valk  
 1051 (Editors), *Tree islands of the Everglades*. Kluwer Academic Publishers, Dordrecht, The  
 1052 Netherlands, pp 19-69.
- 1053 Wintenberger CL, Rodrigues S, Breheret JG, Villar M. 2015. Fluvial islands: First stage of  
 1054 development from nonmigrating (forced) bars and woody-vegetation interactions.  
 1055 *Geomorphology*, 246: 305-320.
- 1056 Wyrick JR, Klingeman PC. 2011. Proposed fluvial island classification scheme and its use  
 1057 for river restoration. *River Research and Applications*, 27(7): 814-825.
- 1058 Zen S, Zolezzi G, Toffolon M, Gurnell AM. 2016. Biomorphodynamic modelling of inner bank  
 1059 advance in migrating river bends. *Advances in Water Resources*, 93: 166-181.

1060

# 1061 **FIGURE UNDERLINES**

- 1062 Figure 1. Distribution of sampling locations used in 2016 and 2017 according to date of  
 1063 surface initiation, overlain on images of the study reach captured in 2002 and 2015. The  
 1064 images are overlain with coordinates for WGS84 UTM zone 33 to indicate the study area  
 1065 location. Images were obtained from Google Earth, Image © 2017 DigitalGlobe, and were  
 1066 captured on 21 July 2002 and 12 July 2015.
- 1067 Figure 2. Data sets and events described in this paper in relation to variations in water level  
 1068 in the study reach between January 2000 and February 2017 inclusive.

Figure 3. Water level (detrended elevation in m) - frequency relationship in the study reach estimated for the period 2000-2017, compared with the interquartile range of the detrended elevation of sampling locations on 1980EI, 2000PI, 2000btwn, 2004PI, 2004btwn surfaces in 2005, 2010 and 2013 and the maximum river stage between June 2016 and February 2017 sampling campaigns.

Figure 4. **Surface** sediment sampling locations and times plotted in relation to their scores on the first two PCs of a PCA. The PCA was applied to the %organic, D50, %gravel, %sand, %silt, %clay content of each sample: (iii) illustrates the loadings of these six variables on the first two PCs. The samples are coded according to (i) the sampled surface, (ii) the survey year, (iv) sediment class (derived from AHC of %organic, D50, %gravel, %sand, %silt, %clay), (v) surface age at the time of sampling.

Figure 5. A, B, C, D: Particle size distributions for the <1 mm ( $0\phi$ ) fraction of island surface (A, B) and unvegetated and between island (CD) **surface** sediment samples obtained in June 2016 (A,C) and February 2017 (B,D). The data are presented as percentages of the sample within  $1\phi$  bins (<1, 1-2, 2-3, ..., 10-11, >11  $\phi$ ). E, F, G: D10, D50 and D90 percentile particle sizes estimated for the 139 distributions contributing to the averages shown in A, B, C, D. Note that some D10 estimates are larger (<0  $\phi$ ) because the <1  $\phi$  bin contains such a large percentage of the particles in these coarse samples.

Figure 6. A. Box plots of canopy height at sampling locations on 1980, 2000 and 2004 island surfaces and between 2000 and 2004 islands, extracted from Lidar surveys captured in 2005, 2010, 2013 and field measurements in 2016 (2000PI, 2004PI only). B. C. D. Some living components of the organic material in island and unvegetated bar surface sediments (1980EI, 2000PI, 2004PI, 2010PI, 2014PI, unveg): A. seeds per m<sup>2</sup> sampled in February 2017, B. total hyphal length sampled in July 2012, C. total root length sampled in May 2012 (data for B and C from Mardhiah et al., 2014).

1  
2  
3 1094 Figure 7. Similarity in the species composition of the standing vegetation (July 2011, June  
4  
5 1095 2016) and seed bank (February 2011) observed on surfaces of different type and age.  
6  
7 1096 Agglomerative Hierarchical Cluster analysis was performed with the Jaccard coefficient as  
8  
9 1097 the similarity measure and clustering determined using the unweighted pair group average.  
10  
11 1098 Figure 8. Standing vegetation and seed bank species composition on surfaces of different  
12  
13 1099 age, based on surveys of the standing vegetation in 2011 and 2016, and the winter seed  
14  
15 1100 bank in 2017. A. Number of species present, B. Average C, S, R scores, C. Proportions of  
16  
17 1101 species with long-term persistent, short-term persistent, and transient seed banks, D.  
18  
19 1102 Proportions of different most common terminal habitats  
20  
21  
22 1103 Figure 9. Daily total precipitation, maximum wind speed, and maximum detrended water  
23  
24 1104 level between field campaigns in June 2016 and February 2017.  
25  
26 1105  
27  
28  
29  
30  
31  
32  
33  
34  
35  
36  
37  
38  
39  
40  
41  
42  
43  
44  
45  
46  
47  
48  
49  
50  
51  
52  
53  
54  
55  
56  
57  
58  
59  
60

1  
2  
3  
4  
5  
6  
7  
8  
9  
10  
11  
12  
13  
14  
15  
16  
17  
18  
19  
20  
21  
22  
23  
24  
25  
26  
27  
28  
29  
30  
31  
32  
33  
34  
35  
36  
37  
38  
39  
40  
41  
42  
43  
44  
45  
46  
47  
48  
49  
50  
51  
52  
53  
54  
55  
56  
57  
58  
59  
60

**TABLES**

Table 1. Generalised linear models for detrended surface elevation and vegetation canopy height in relation to sampled surfaces (1980EI, 2000PI, 2000btwn, 2004PI, 2004btwn) Lidar survey years (2013, 2010, 2005) and interactions between surfaces and years

	DF	F-value	P-value	Bonferroni pairwise comparisons (P<0.05)
<b>Bed elevation</b>				
Surface	4	77.60	<0.001	1980EI > 2000PI, 2000btwn > 2004PI, 2004btwn
Lidar date	2	3.55	0.031	2013, 2010 > 2005
R <sup>2</sup> (adjusted) = 65.8%				
<b>Vegetation Canopy</b>				
Surface	4	940.62	<0.001	1980EI > 2000PI > 2004PI > 2000btwn,2004btwn
Lidar date	2	64.24	<0.001	2013 > 2010 > 2005
Surface*Lidar date	8	8.99	<0.001	1980EI(2013,2010,2005) > 2000PI(2013) > 2000PI(2010),2004PI(2013) > 2004PI(2010) > 2000PI(2005),2000btwn(2013,2010,2005),2004PI(2005), 2004btwn(2013,2010,2005)
R <sup>2</sup> (adjusted) = 96.36%				



1112 Table 2. Centroid values for sediment classes discriminated using AHC (Euclidean distance,  
 1113 Ward's clustering algorithm) applied to six sediment properties of 139 **surface** sediment  
 1114 samples, with significant differences between classes in relation to the six contributing  
 1115 sediment properties (Kruskal Wallis tests).

Sample size and sediment property	A mainly gravel	B gravel-sand	C sand-gravel	D mainly sand (notable organic)	E sand with some silt (notable organic)	F sand-silt (notable organic and clay)	Significant differences between classes*
sample size	23	25	16	36	28	41	
%organic	0.3	0.8	1.4	5.0	4.8	6.0	D,E,F>A,B C>A
D50( $\phi$ )	-1.4	-1.7	1.3	2.1	2.9	3.7	E,F>C,D>A,B
%gravel	80.6	58.5	26.3	0.5	0.4	0.1	A,B,C>D,E,F A>C
%sand	19.0	38.5	64.9	91.0	76.8	59.8	C,D,E,F >A,B D>C,F
%silt	0.5	2.9	8.4	8.4	21.7	37.5	E,F>B,C,D>A C,D>B
%clay	0.0	0.1	0.4	0.1	1.2	2.7	E,F>A,B,C,D

1116 \* Kruskal Wallis tests, df = 5, P < 0.0001, multiple pairwise comparisons using Dunn's  
 1117 procedure with Bonferroni corrected significance level (P = 0.003)

1118

1  
2  
3 1119  
4  
5 1120  
6  
7 1121  
8  
9 1122  
10  
11  
12  
13  
14  
15  
16  
17  
18  
19  
20  
21  
22  
23  
24  
25  
26  
27  
28  
29  
30  
31  
32  
33 1123  
34  
35 1124  
36  
37  
38  
39  
40  
41  
42  
43  
44  
45  
46  
47  
48  
49  
50  
51  
52  
53  
54  
55  
56  
57  
58  
59  
60

Table 3. Eigenvalues, percentage variability explained, and variable loadings on the first three Principal Components of a PCA applied to six sediment properties of 139 surface sediment samples.

	PC1	PC2	PC3
Eigenvalue	4.371	1.201	0.197
Variability (%)	72.843	20.010	3.282
Cumulative %	72.843	92.854	96.136
Loadings			
%organic	0.921	0.157	-0.336
D50( $\phi$ )	0.946	-0.123	0.161
%gravel	-0.937	-0.280	0.001
%sand	0.568	0.790	0.182
%silt	0.926	-0.304	-0.059
%clay	0.754	-0.605	0.146

Table 4. Generalised linear models for each of the ten, fifty and ninety percentiles (D10, D50, D90) of the 0  $\phi$  and finer mineral sediment fraction of 139 particle size distributions, with sampling year (2016, 2017), surface (1980EI, 2000PI, 2000btwn, 2004PI, 2004btwn, 2014PI, unveg) and interactions between year and surface as the explanatory variables (percentile expressed in  $\phi$  units, statistical significance of differences between groups explored using the Bonferroni method).

	DF	F-value	P-value	Bonferroni pairwise comparisons (P<0.05)
<b>D10</b>				
Surface	6	44.27	<0.001	1980EI, 2000PI, 2004PI > 2014PI, 2000btwn > 2004btwn, unveg
Year	1	8.51	0.004	2017 > 2016
			R <sup>2</sup> (adjusted) = 66.8%	
<b>D50</b>				
Surface	6	35.11	<0.001	1980EI, 2000PI, 2004PI > 2014PI, 2000btwn > 2004btwn, unveg
Year	1	8.88	0.003	2017 > 2016
			R <sup>2</sup> (adjusted) = 60.6%	
<b>D90</b>				
Surface	6	26.00	<0.001	1980EI, 2000PI, 2004PI > 2000btwn, 2004btwn > unveg 2014PI > unveg
Year	1	9.37	0.003	2017 > 2016
Surface*Year	6	5.41	<0.001	1980EI(2016,2017), 2000PI(2016,2017), 2004PI(2016, 2017), 2014PI(2017), 2000btwn(2017), 2004btwn(2017) > 2000btwn(2016), 2004btwn(2016), unveg(2016,2017)
			R <sup>2</sup> (adjusted) = 57.2%	

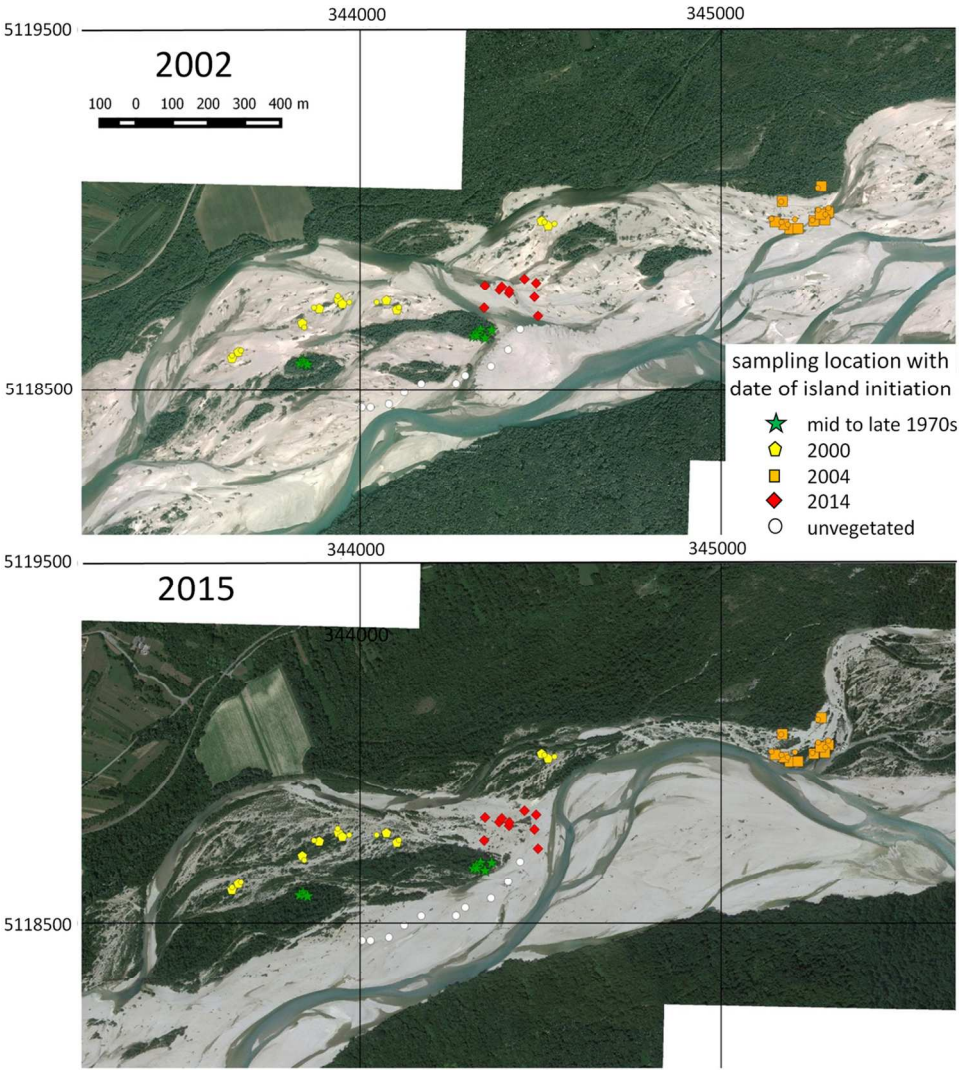


Figure 1. Distribution of sampling locations used in 2016 and 2017 according to date of surface initiation, overlain on images of the study reach captured in 2002 and 2015. The images are overlain with coordinates for WGS84 UTM zone 33 to indicate the study area location. Images were obtained from Google Earth, Image © 2017 DigitalGlobe, and were captured on 21 July 2002 and 12 July 2015.

113x122mm (300 x 300 DPI)

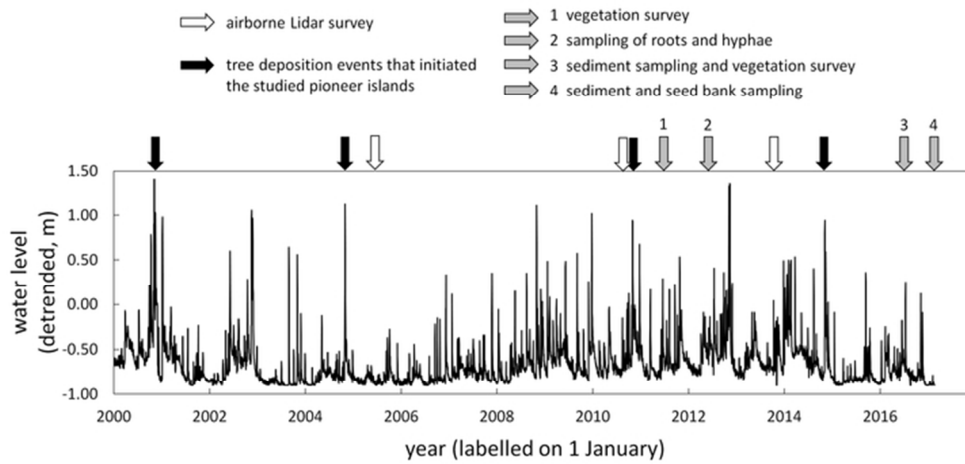


Figure 2. Data sets and events described in this paper in relation to variations in water level in the study reach between January 2000 and February 2017 inclusive.

62x29mm (300 x 300 DPI)

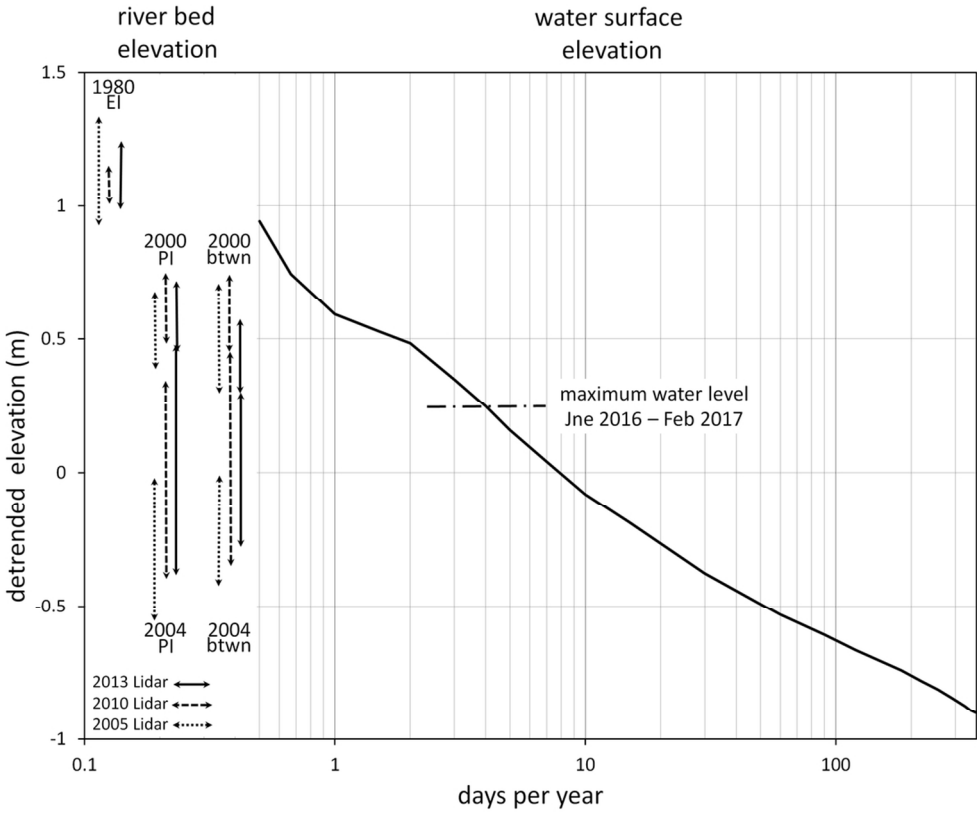


Figure 3. Water level (detrended elevation in m) - frequency relationship in the study reach estimated for the period 2000-2017, compared with the interquartile range of the detrended elevation of sampling locations on 1980EI, 2000PI, 2000btwn, 2004PI, 2004btwn surfaces in 2005, 2010 and 2013 and the maximum river stage between June 2016 and February 2017 sampling campaigns.

103x84mm (300 x 300 DPI)

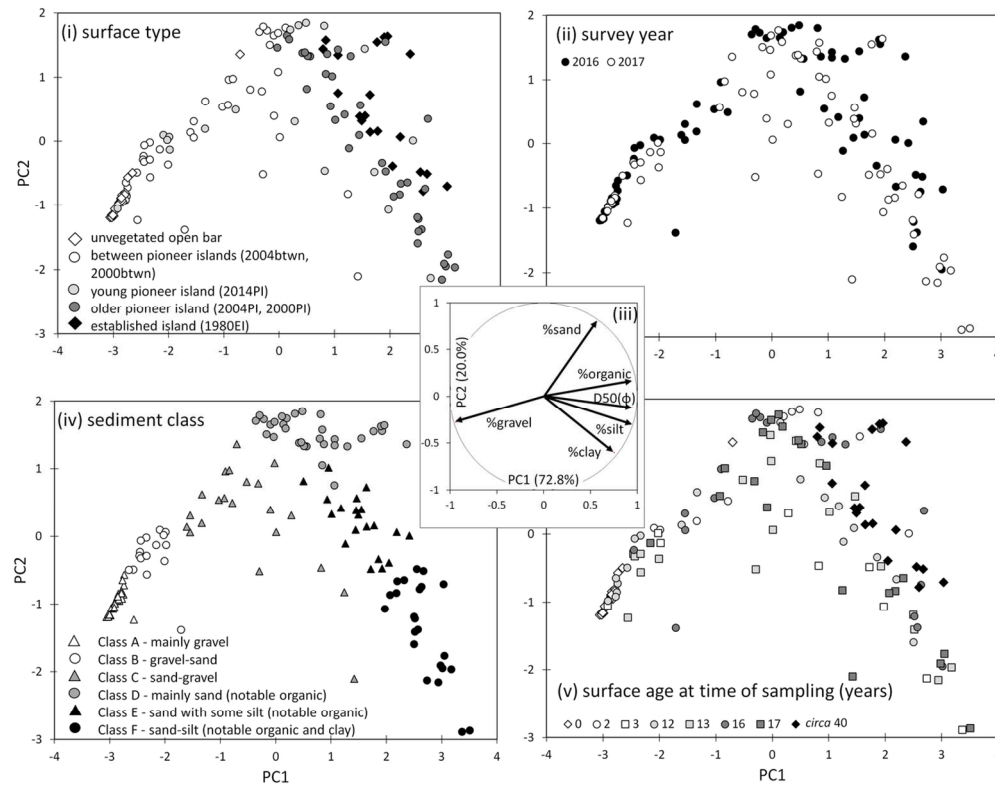


Figure 4. Sediment sampling locations and times plotted in relation to their scores on the first two PCs of a PCA. The PCA was applied to the %organic, D50, %gravel, %sand, %silt, %clay content of each sample: (iii) illustrates the loadings of these six variables on the first two PCs. The samples are coded according to (i) the sampled surface, (ii) the survey year, (iv) sediment class (derived from AHC of %organic, D50, %gravel, %sand, %silt, %clay), (v) surface age at the time of sampling.

124x100mm (300 x 300 DPI)



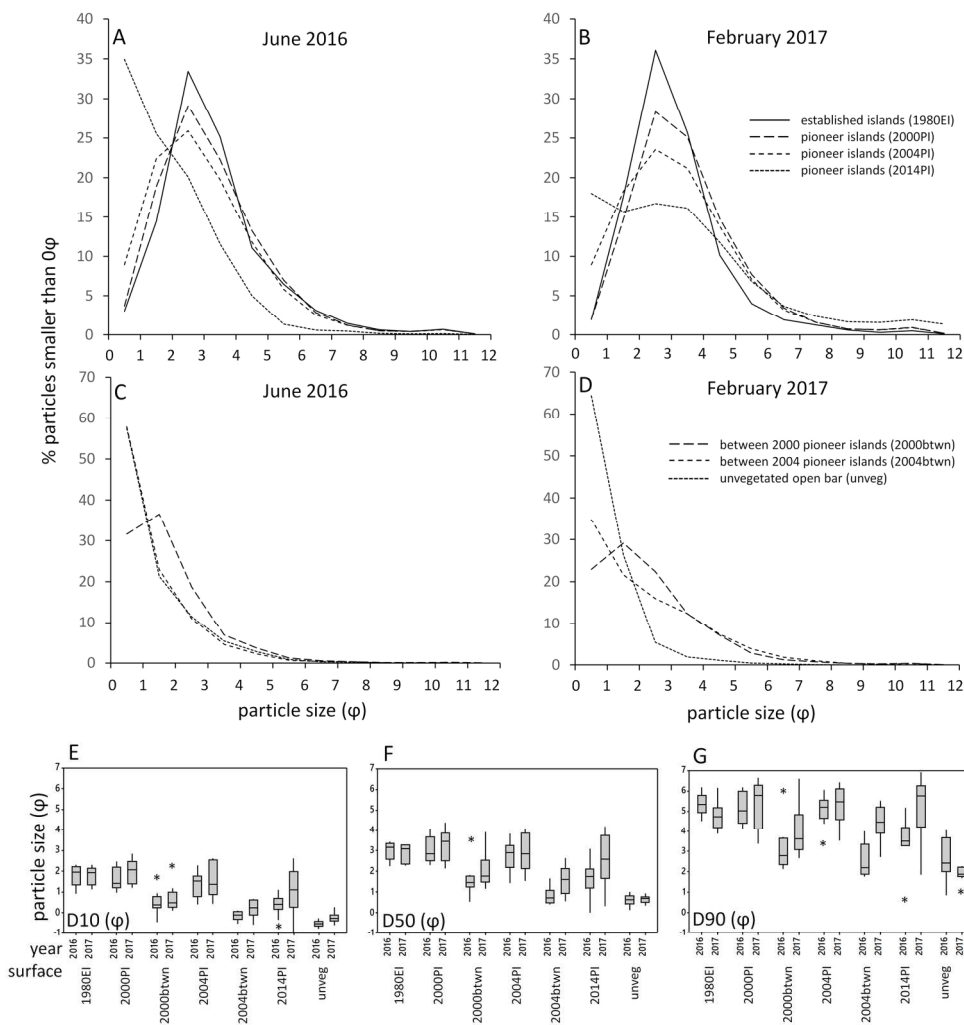


Figure 5. A, B, C, D: Particle size distributions for the <1 mm ( $0 \phi$ ) fraction of island surface (A, B) and unvegetated and between island (C, D) sediment samples obtained in June 2016 (A,C) and February 2017 (B,D). The data are presented as percentages of the sample within 1  $\phi$  bins (<1, 1-2, 2-3, ..., 10-11, >11  $\phi$ ). E, F, G: D10, D50 and D90 percentile particle sizes estimated for the 139 distributions contributing to the averages shown in A, B, C, D. Note that some D10 estimates are larger (<0  $\phi$ ) because the <1  $\phi$  bin contains such a large percentage of the particles in these coarse samples.

168x173mm (300 x 300 DPI)

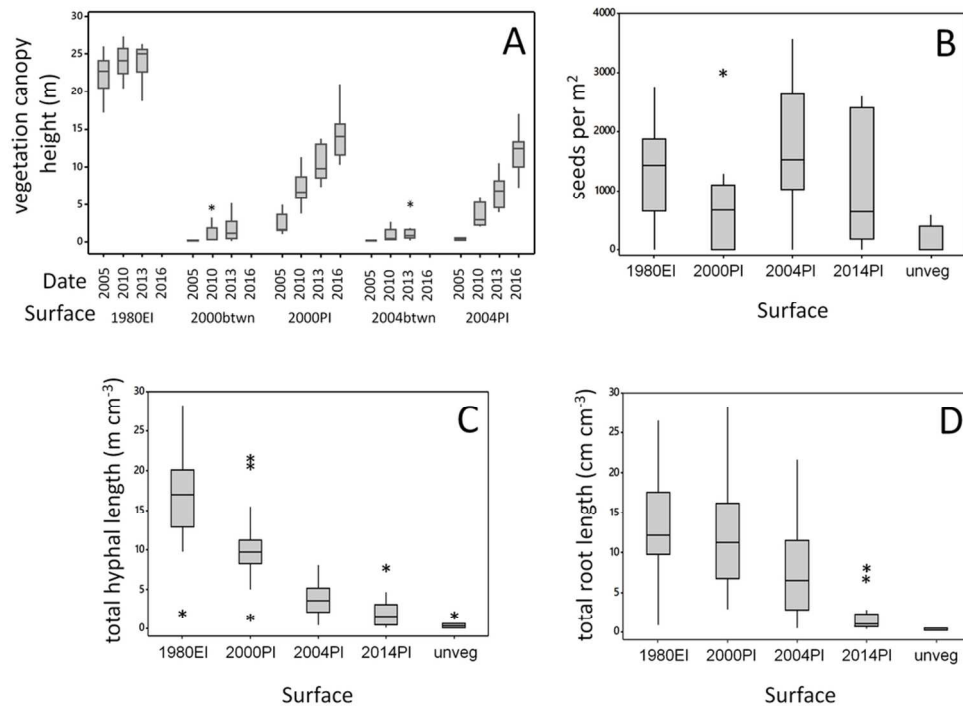


Figure 6. A. Box plots of canopy height at sampling locations on 1980, 2000 and 2004 island surfaces and between 2000 and 2004 islands, extracted from Lidar surveys captured in 2005, 2010, 2013 and field measurements in 2016 (2000PI, 2004PI only). B. C. D. Some living components of the organic material in island and unvegetated bar surface sediments (1980EI, 2000PI, 2004PI, 2010PI, 2014PI, unveg): A. seeds per m<sup>2</sup> sampled in February 2017, B. total hyphal length sampled in July 2012, C. total root length sampled in May 2012 (data for B and C from Mardhiah et al., 2014).

94x69mm (300 x 300 DPI)

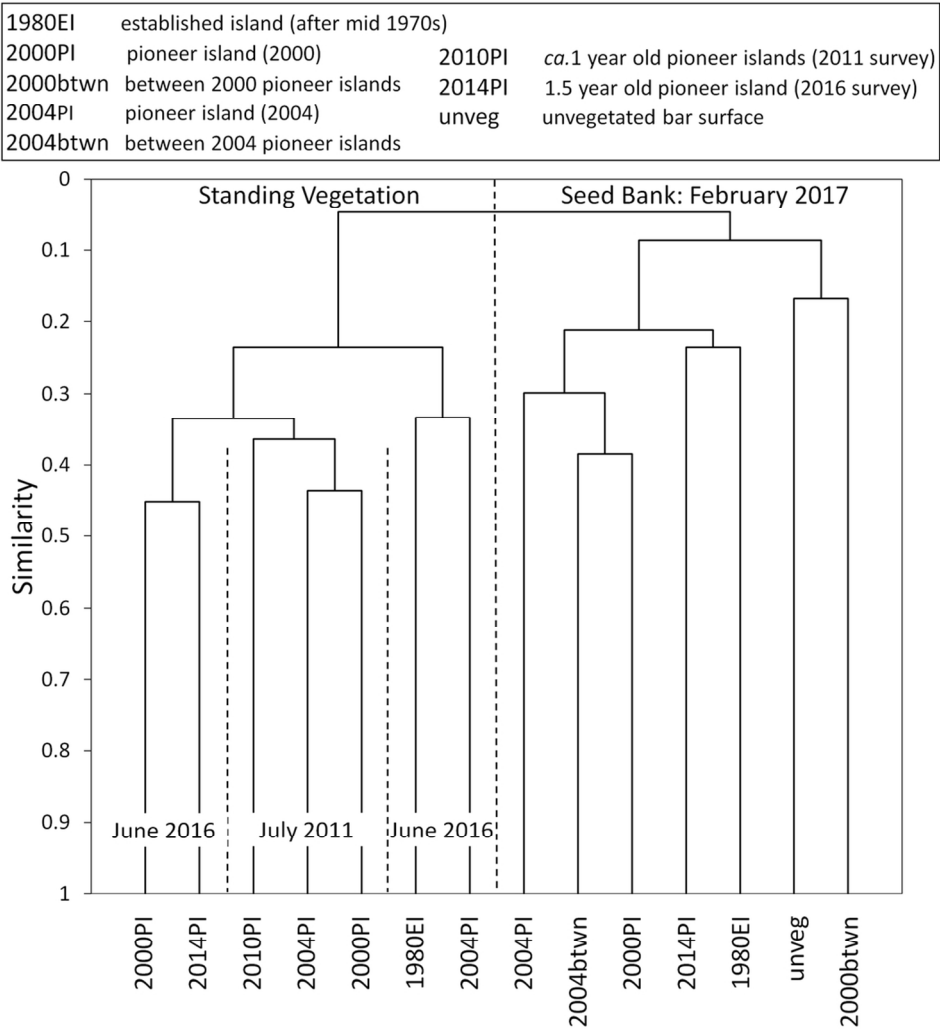


Figure 7. Similarity in the species composition of the standing vegetation (July 2011, June 2016) and seed bank (February 2011) observed on surfaces of different type and age. Agglomerative Hierarchical Cluster analysis was performed with the Jaccard coefficient as the similarity measure and clustering determined using the unweighted pair group average.

104x108mm (300 x 300 DPI)

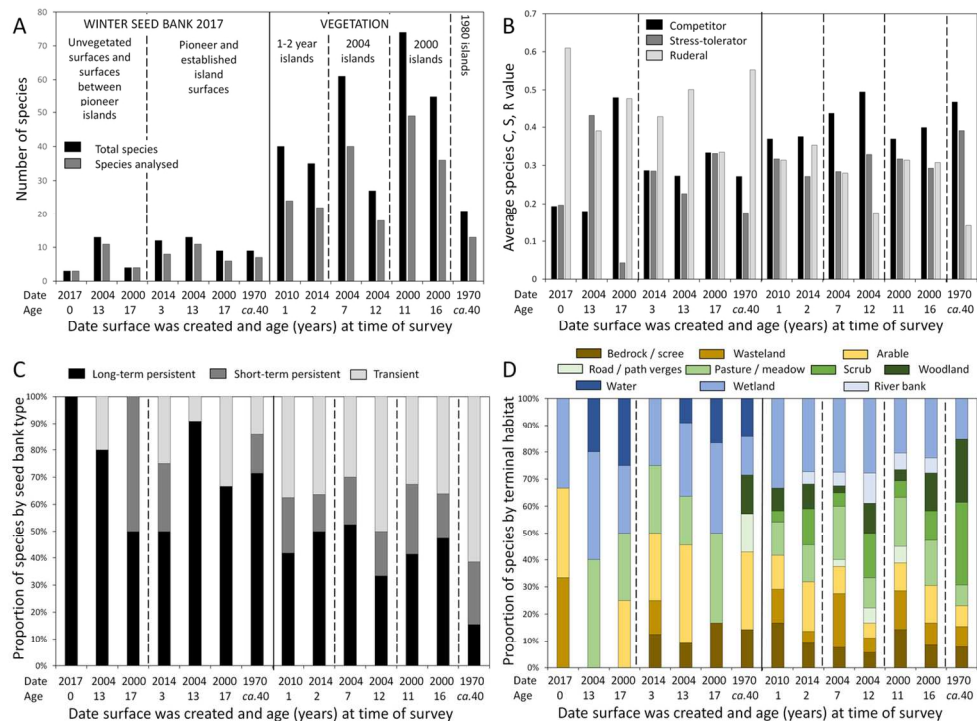


Figure 8. Standing vegetation and seed bank species composition on surfaces of different age, based on surveys of the standing vegetation in 2011 and 2016, and the winter seed bank in 2017. A. Number of species present, B. Average C, S, R scores, C. Proportions of species with long-term persistent, short-term persistent, and transient seed banks, D. Proportions of different most common terminal habitats

124x93mm (300 x 300 DPI)

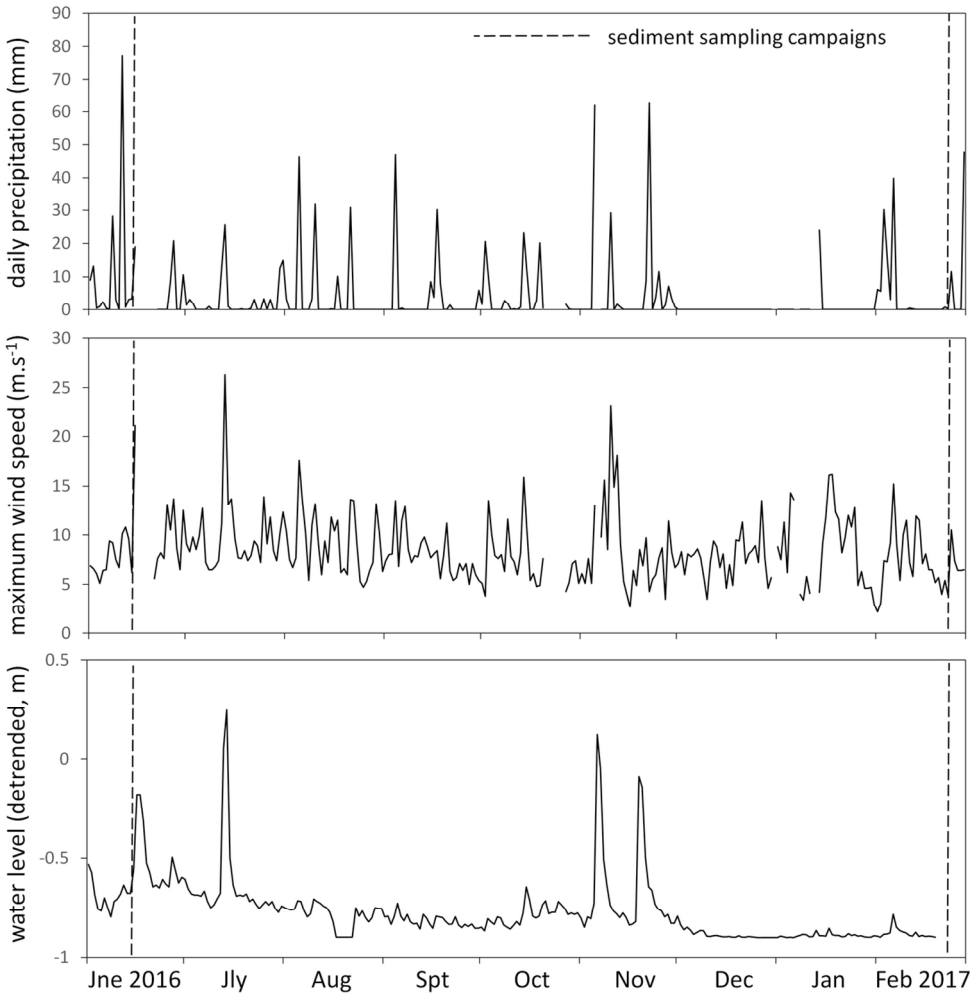


Figure 9. Daily total precipitation, maximum wind speed, and maximum detrended water level between field campaigns in June 2016 and February 2017.

119x121mm (300 x 300 DPI)